



HAL
open science

FOKKER-PLANCK MULTI-SPECIES EQUATIONS IN THE ADIABATIC ASYMPTOTICS

Francis Filbet, Claudia Negulescu

► **To cite this version:**

Francis Filbet, Claudia Negulescu. FOKKER-PLANCK MULTI-SPECIES EQUATIONS IN THE ADIABATIC ASYMPTOTICS. 2022. hal-03573120v3

HAL Id: hal-03573120

<https://hal.science/hal-03573120v3>

Preprint submitted on 20 Sep 2022

HAL is a multi-disciplinary open access archive for the deposit and dissemination of scientific research documents, whether they are published or not. The documents may come from teaching and research institutions in France or abroad, or from public or private research centers.

L'archive ouverte pluridisciplinaire **HAL**, est destinée au dépôt et à la diffusion de documents scientifiques de niveau recherche, publiés ou non, émanant des établissements d'enseignement et de recherche français ou étrangers, des laboratoires publics ou privés.

FOKKER-PLANCK MULTI-SPECIES EQUATIONS IN THE ADIABATIC ASYMPTOTICS

FRANCIS FILBET AND CLAUDIA NEGULESCU

ABSTRACT. The main concern of the present paper is the study of the multi-scale dynamics of thermonuclear fusion plasmas via a multi-species Fokker-Planck kinetic model. One of the goals is the generalization of the standard Fokker-Planck collision operator to a multi-species one, conserving mass, total momentum and energy, as well as satisfying Boltzmann's H -theorem. Secondly, we perform on one hand a mathematical asymptotic limit, letting the electron/ion mass ratio converging towards zero, to obtain a thermodynamic equilibrium state for the electrons (adiabatic regime), whereas the ions are kept kinetic. On the other hand, we develop a first numerical scheme, based on a Hermite spectral method, and perform numerical simulations to investigate in more details this asymptotic limit.

Keywords: Plasma modelling, Fokker-Planck kinetic equations, adiabatic electron regime, asymptotic analysis, entropy-methods, multi-scale numerical scheme.

CONTENTS

1. Introduction	1
2. The mixed kinetic model and its scaling	3
2.1. The mixed kinetic model	3
2.2. Characteristic scales and regime of interest	5
2.3. Non-dimensional kinetic system	6
3. Formal derivation of the asymptotic model	9
4. Numerical scheme	16
4.1. Hermite expansion for the electron system	16
4.2. Space/time discretization	20
4.3. Adaptive algorithm for Hermite coefficients	23
5. Numerical simulations	23
5.1. One species case	24
5.2. Two species case	25
6. Concluding remarks and perspectives	31
References	33

1. INTRODUCTION

Starting with the first projects born in Russia in the early 1950's, continuous efforts were made to produce clean and reliable energy in tokamak fusion reactors able to confine a very hot plasma gas via strong electromagnetic fields. The mathematical modelling is a useful tool in this process. Kinetic models, based on a mesoscopic description of the various particles constituting a plasma, and coupled to Maxwell's equations for the computation of the

electromagnetic fields, are very precise approaches for the study of such thermonuclear fusion plasmas. However, treating each species in a kinetic framework is computationally very demanding, such that approximate models have been introduced. Especially when one is interested in the investigation of phenomena occurring on the (slow) ion scales, electrons are approximated via macroscopic models (adiabatic models). The justification is that the time- and length-scales associated with the electrons are very small as compared to the ones of the ions (due to the small mass ratio m_e/m_i), such that electrons are considered to be in a thermodynamic equilibrium. Such hybrid strategies, treating ions in a fully kinetic manner and electrons via fluid approaches, are often used in today's simulations [6, 8, 19, 31], leading to significant savings in computational time and memory. But, describing particles via a fluid model requires that the electron distribution function remains close to a thermodynamic equilibrium, meaning being close to a Maxwellian distribution in the velocity variable. Coulomb collisions in a thermonuclear plasma are however not sufficiently effective to thermalize the electrons. Thus, the validity of the adiabatic electron model (electron Boltzmann relation) is rather controversial. Indeed, this model seems to break down in various situations, as for example in the edge plasma region, or it does not take into account for important instabilities, such as the Trapped Electron Modes (TEM), which are considered as essential in the turbulent dynamics [14].

In this paper, we shall especially focus on the asymptotic towards the electron Boltzmann regime, starting from a kinetic picture where collisions and collective effects (electrostatic forces) are well balanced. To investigate this dynamic, we are firstly introducing a multi-species Fokker-Planck equations, with particular emphasize on the inter-species collision operators and their properties. In the literature one can find various simplified models for inter-species collisions. For instance BGK models for gas mixtures are given as a sum of relaxation operators. One example is the model of Klingenberg, Pirner and Puppo [30] or Bobylev, Bisi, Groppi, Spiga and Potapenko [3]. It contains the often used models of Gross and Krook [23, 24] and Hamel [26] as special cases. Other type of models contain only one collision term on the right-hand side as the one proposed by Andries, Aoki and Perthame in [1]. In this paper we focus on Fokker-Planck type operators which are more consistent for the description of collisional plasmas [11, 35, 10, 12]. The model is derived by introducing mixed temperatures and momenta, under the constraint that the number of particles of each species, the total momentum and the total energy are conserved. Moreover, we prove that the model satisfies an H-Theorem, permitting to characterize the form of equilibrium.

Having introduced these Fokker-Planck collision operators, a physical scaling is performed permitting to characterize the regime of interest in our plasma studies, namely focusing on the ion dynamics. This allows to identify a small parameter $\varepsilon \ll 1$ which shall permit to obtain the desired electron Boltzmann relation, when performing a formal asymptotic limit $\varepsilon \rightarrow 0$. Our main goal is to design a numerical method able to give precise results for all values of $\varepsilon \in [0, 1]$, especially able to follow the asymptotic limit $\varepsilon \rightarrow 0$ without extensive numerical efforts. The idea is to have a scheme which can treat electrons and ions simultaneously without having to adapt the mesh to the different species, but rather to the physical phenomenon one wants to investigate. In this aim we shall present in this paper the first step towards such a performant scheme, based on a Hermite spectral approach to cope with the velocity variable [16, 17, 34]. Hermite spectral methods offer indeed an ideal way to perform large-scale simulations, including at the same time microscopic kinetic effects. The choice of a suitable scaling of the Hermite basis functions, adapted to the investigated asymptotic, is fundamental, rendering the Hermite approach intrinsically multiscale and providing thus a

natural bridge between the microscopic and the macroscopic worlds. Indeed, in the limit $\varepsilon \rightarrow 0$, the distribution function can be represented by only one Hermite function, reducing drastically the number of discretization parameters in the velocity space. The use of Hermite functions for the resolution of kinetic equations was proposed for the first time by Grad in [22].

At the end of this work numerical simulations are presented in the aim to show the advantage of such a Hermite spectral approach, in particular to understand how the electron distribution function converges after a transient regime towards its thermodynamic limit in the context of plasma simulations. The specificity of this method will be underlined, namely the fact that it permits considerable improvements in simulation time for small ε -values, as in such regimes very few Hermite modes have to be taken into account.

The outline of this paper is the following. In Section 2 we present the fully kinetic ion-electron model and its physical scaling leading to a multi-scale multi-species coupled Fokker-Planck model. Section 3 deals with the formal derivation of the hybrid limit-model, when letting a small parameter $\varepsilon \ll 1$ tend towards zero, parameter standing somehow for the small electron-to-ion mass ratio. The well-posedness of the limit-model is also investigated. And finally in Sections 4 and 5 we shall present a first numerical scheme, based on a Hermite spectral approach, and shall conclude with the study of some numerical simulations.

2. THE MIXED KINETIC MODEL AND ITS SCALING

2.1. The mixed kinetic model. The starting point of this work is the following model composed of two coupled kinetic equations for the ions respectively electrons of a fusion plasma, *i.e.*

$$(2.1) \quad \begin{cases} \partial_t f_i + \mathbf{v} \cdot \nabla_{\mathbf{x}} f_i + \frac{e}{m_i} \mathbf{E} \cdot \nabla_{\mathbf{v}} f_i = \mathcal{Q}_{ii}(f_i, f_i) + \mathcal{Q}_{ie}(f_i, f_e), \\ \partial_t f_e + \mathbf{v} \cdot \nabla_{\mathbf{x}} f_e - \frac{e}{m_e} \mathbf{E} \cdot \nabla_{\mathbf{v}} f_e = \mathcal{Q}_{ee}(f_e, f_e) + \mathcal{Q}_{ei}(f_e, f_i), \end{cases}$$

associated to Poisson's equation for the description of the electrostatic potential

$$(2.2) \quad -\Delta\phi = \frac{e}{\varepsilon_0} (n_i - n_e), \quad \mathbf{E} = -\nabla_{\mathbf{x}}\phi,$$

with e the elementary charge, m_α the mass of species $\alpha \in \{e, i\}$ and ε_0 the vacuum permittivity. The magnetic field \mathbf{B} is not considered here, as we shall focus in the following rather on the dynamics parallel to \mathbf{B} and did not want to encumber the paper. For a more general framework see [32]. The functions $f_\alpha(t, \mathbf{x}, \mathbf{v})$ represent the particle distribution functions in the phase-space $(\mathbf{x}, \mathbf{v}) \in \mathbb{T}^d \times \mathbb{R}^d$ (\mathbb{T}^d being the d -dimensional torus) whereas the electron and ion macroscopic quantities are given for $\alpha \in \{e, i\}$ by

$$\left\{ \begin{array}{l} n_\alpha(t, \mathbf{x}) := \int_{\mathbb{R}^d} f_\alpha(t, \mathbf{x}, \mathbf{v}) \, d\mathbf{v}, \\ n_\alpha \mathbf{u}_\alpha(t, \mathbf{x}) := \int_{\mathbb{R}^d} \mathbf{v} f_\alpha(t, \mathbf{x}, \mathbf{v}) \, d\mathbf{v}, \\ dk_B n_\alpha T_\alpha(t, \mathbf{x}) := m_\alpha \int_{\mathbb{R}^d} |\mathbf{v} - \mathbf{u}_\alpha|^2 f_\alpha(t, \mathbf{x}, \mathbf{v}) \, d\mathbf{v}, \\ w_\alpha(t, \mathbf{x}) := \frac{m_\alpha}{2} \int_{\mathbb{R}^d} |\mathbf{v}|^2 f_\alpha(t, \mathbf{x}, \mathbf{v}) \, d\mathbf{v} = \frac{d}{2} k_B n_\alpha T_\alpha + \frac{m_\alpha}{2} n_\alpha |\mathbf{u}_\alpha|^2, \end{array} \right.$$

with k_B the Boltzmann constant. The collision operators describing the inter- and intra-species interactions are chosen of Fokker-Planck type, *i.e.* given for $\alpha, \beta \in \{e, i\}$ by

$$\mathcal{Q}_{\alpha\beta}(f_\alpha, f_\beta) := \nu_{\alpha\beta} \operatorname{div}_{\mathbf{v}} \left((\mathbf{v} - \mathbf{u}_{\alpha\beta}) f_\alpha + \frac{k_B T_{\alpha\beta}}{m_\alpha} \nabla_{\mathbf{v}} f_\alpha \right),$$

where $\nu_{\alpha\beta} > 0$ are the collisional frequencies corresponding to the couple (α, β) of particles.

For intra-species collisions, we have $\mathbf{u}_{\alpha\alpha} := \mathbf{u}_\alpha$, $T_{\alpha\alpha} := T_\alpha$ and the collision operator $\mathcal{Q}_{\alpha\alpha}(f_\alpha, f_\alpha)$ is chosen in such a way to get conservation of mass, momentum and kinetic energy

$$m_\alpha \int_{\mathbb{R}^d} \mathcal{Q}_{\alpha\alpha}(f_\alpha, f_\alpha) \begin{pmatrix} 1 \\ \mathbf{v} \\ \frac{|\mathbf{v}|^2}{2} \end{pmatrix} d\mathbf{v} = 0, \quad \forall \alpha \in \{e, i\},$$

as well as the entropy decay

$$\int_{\mathbb{R}^d} \mathcal{Q}_{\alpha\alpha}(f_\alpha, f_\alpha) \ln(f_\alpha) d\mathbf{v} \leq 0, \quad \forall \alpha \in \{e, i\},$$

leading to the thermal equilibrium

$$\int_{\mathbb{R}^d} \mathcal{Q}_{\alpha\alpha}(f_\alpha, f_\alpha) \ln(f_\alpha) d\mathbf{v} = 0 \iff f_\alpha = \mathcal{M}_{n_\alpha, \mathbf{u}_\alpha, T_\alpha},$$

where $\mathcal{M}_{n_\alpha, \mathbf{u}_\alpha, T_\alpha}$ is the local Maxwellian defined by

$$(2.3) \quad \mathcal{M}_{n_\alpha, \mathbf{u}_\alpha, T_\alpha}(\mathbf{v}) := n_\alpha \left(\frac{m_\alpha}{2\pi k_B T_\alpha} \right)^{d/2} \exp \left(-m_\alpha \frac{|\mathbf{v} - \mathbf{u}_\alpha|^2}{2k_B T_\alpha} \right).$$

However for the inter-species collisions the situation is more complex. The choice of the inter-species mixed velocities $\mathbf{u}_{\alpha\beta}$ and temperatures $T_{\alpha\beta}$ is done such that to enforce the appropriate conservation laws and to ensure the H-theorem. For this we shall first of all require that

$$(2.4) \quad \mathbf{u}_{\alpha\beta} = \mathbf{u}_{\beta\alpha}, \quad T_{\alpha\beta} = T_{\beta\alpha}, \quad \nu_{ei} m_e n_e = \nu_{ie} m_i n_i.$$

These three requirements are fundamental and also physical. The justification of the last assumption comes from the Coulomb collisional frequency [28], given by

$$\nu_{\alpha\beta} = C e_\alpha^2 e_\beta^2 n_\beta \frac{m_\beta}{m_\alpha + m_\beta} \frac{1}{(v_{th,\alpha}^2 + v_{th,\beta}^2)^{3/2}}, \quad C > 0.$$

With these assumptions and the fact that we would like to ensure the total momentum conservation

$$m_e \int_{\mathbb{R}^d} \mathcal{Q}_{ei}(f_e, f_i) \mathbf{v} d\mathbf{v} + m_i \int_{\mathbb{R}^d} \mathcal{Q}_{ie}(f_i, f_e) \mathbf{v} d\mathbf{v} = 0,$$

the total kinetic energy conservation

$$m_e \int_{\mathbb{R}^d} \mathcal{Q}_{ei}(f_e, f_i) \frac{|\mathbf{v}|^2}{2} d\mathbf{v} + m_i \int_{\mathbb{R}^d} \mathcal{Q}_{ie}(f_i, f_e) \frac{|\mathbf{v}|^2}{2} d\mathbf{v} = 0,$$

as well as the global entropy decay

$$\int_{\mathbb{R}^d} \mathcal{Q}_{ei}(f_e, f_i) \ln(f_e) d\mathbf{v} + \int_{\mathbb{R}^d} \mathcal{Q}_{ie}(f_i, f_e) \ln(f_i) d\mathbf{v} \leq 0,$$

a unique choice of mixed velocities is possible, given by

$$(2.5) \quad \mathbf{u}_{ei} = \mathbf{u}_{ie} := \frac{\mathbf{u}_e + \mathbf{u}_i}{2},$$

as well as a unique choice of mixed temperatures, namely

$$(2.6) \quad T_{ei} = T_{ie} := \frac{m_i T_e + m_e T_i}{m_e + m_i} + \frac{m_i m_e}{m_i + m_e} \frac{|\mathbf{u}_e - \mathbf{u}_i|^2}{2d k_B}.$$

To simplify the computations, let us remark that the collision operators can be rewritten in a simpler form as follows

$$\mathcal{Q}_{\alpha\beta}(f_\alpha, f_\beta) = \nu_{\alpha\beta} \operatorname{div}_{\mathbf{v}} \left(\frac{k_B T_{\alpha\beta}}{m_\alpha} \mathcal{M}_{\alpha\beta} \nabla_{\mathbf{v}} \left(\frac{f_\alpha}{\mathcal{M}_{\alpha\beta}} \right) \right),$$

with $\mathcal{M}_{\alpha\beta}$ the local Maxwellian given by

$$(2.7) \quad \mathcal{M}_{\alpha\beta}(t, \mathbf{x}, \mathbf{v}) := n_\alpha(t, \mathbf{x}) \left(\frac{m_\alpha}{2\pi k_B T_{\alpha\beta}(t, \mathbf{x})} \right)^{d/2} \exp \left(-m_\alpha \frac{|\mathbf{v} - \mathbf{u}_{\alpha\beta}(t, \mathbf{x})|^2}{2k_B T_{\alpha\beta}(t, \mathbf{x})} \right).$$

Unlike Boltzmann's operators for neutral gases, the Fokker-Planck operator expresses the cumulative effects of many grazing collisions (rather than short-range collisions), and this is due to the long-range effect of the Coulomb interactions. Thus Fokker-Planck operators describe mainly a diffusion in the velocity space.

2.2. Characteristic scales and regime of interest. Let us now identify some small parameters, characterizing the adiabatic regime of plasma dynamics. This shall be done by firstly introducing the orders of magnitude of the quantities involved in the description of the phenomenon we want to analyse, in our particular case phenomena occurring at the ion spatio-temporal scales.

We start with the microscopic quantities and introduce our first parameter ε , as the mass ratio of electrons and ions

$$\varepsilon^2 := \frac{m_e}{m_i} \ll 1.$$

Next we suppose that the temperatures of electrons and ions are of the same order \bar{T}

$$T_i = \bar{T} T'_i, \quad T_e = \bar{T} T'_e, \quad T_{\alpha\beta} = \bar{T} T'_{\alpha\beta},$$

meaning that the thermal (microscopic) speeds of the two species are widely different and scale as

$$\bar{v}_i := v_{th,i} = \sqrt{\frac{k_B \bar{T}}{m_i}}, \quad \bar{v}_e := v_{th,e} = \sqrt{\frac{k_B \bar{T}}{m_e}} = \frac{1}{\varepsilon} \bar{v}_i.$$

Furthermore we shall assume that the electric and thermal energies are of the same order of magnitude, permitting thus to scale the electric potential as $e \bar{\phi} = k_B \bar{T}$. We also suppose that the plasma is quasineutral, that is, densities of electrons and ions are of the same order \bar{n}

$$n_i = \bar{n} n'_i, \quad n_e = \bar{n} n'_e,$$

permitting thus to fix the magnitude of the ion plasma frequency ω_p and of the Debye length λ_D as

$$\omega_p^{-1} := \sqrt{\frac{\bar{n} e^2}{\varepsilon_0 m_i}}, \quad \lambda_D := \sqrt{\frac{\varepsilon_0 k_B \bar{T}}{\bar{n} e^2}},$$

which yields the relation $\bar{v}_i = \lambda_D \omega_p$.

At the microscopic level again, we fix a time-scale τ_c and a length-scale l_c , related to the ionic collisional process, namely

$$\tau_c := \tau_{ii} = \nu_{ii}^{-1}, \quad l_c := \bar{v}_i \tau_c,$$

where τ_{ii} corresponds to the elapsed time between two ionic collisions (collisional frequency ν_{ii}) and l_c is the corresponding mean free path.

Finally, let us turn to the macroscopic quantities corresponding to the physical device. The macroscopic space-scale \bar{x} is fixed as the distance of interest and the time-scale corresponds to the observation time given by $\bar{t} = \bar{x}/\bar{v}_i$, hence we set for the macroscopic velocities $\bar{u}_\alpha := \bar{v}_\alpha$ as well as $\bar{u}_{ei} = \bar{u}_{ie} = \bar{u}_e$.

To characterize the regime of interest, let us introduce now a second parameter τ as the ratio between micro and macro time-scales

$$\tau := \frac{\tau_c}{\bar{t}}$$

and a third parameter λ as the ratio between micro and macro space-scales

$$\lambda := \frac{\lambda_D}{\bar{x}} = \frac{\bar{v}_i}{\bar{x}} \frac{1}{\omega_p} = \frac{1}{\omega_p \bar{t}}.$$

Concerning the different intra- and inter-species collision frequencies, we simply set

$$\nu_{\alpha\beta} = \bar{\nu}_{\alpha\beta} \nu'_{\alpha\beta}, \quad \forall \alpha, \beta \in \{e, i\},$$

with the order-relations given by [21]

$$\bar{\nu}_{ie} : \bar{\nu}_{ii} : \bar{\nu}_{ee} : \bar{\nu}_{ei} = \varepsilon^2 : \varepsilon : 1 : 1.$$

Finally let us also fix characteristic scales for the distribution functions and the collision operators

$$\bar{f}_\alpha = \frac{\bar{n}}{\bar{v}_\alpha}, \quad \bar{Q}_{\alpha\beta} = \bar{\nu}_{\alpha\beta} \bar{f}_\alpha.$$

The units or scales chosen here are adapted to the plasma regimes we want to study (electron Boltzmann regime). The reader not so familiar with the physics of tokamak fusion plasmas and its characteristic scales is referred to the introductory books [7, 20, 21, 27].

2.3. Non-dimensional kinetic system. Let us observe that we have now a set of three independent parameters $(\varepsilon, \tau, \lambda)$, which characterize several plasma regimes. To get the non-dimensional system, let us perform the following change of variables in the starting model (2.1)

$$\mathbf{x} = \bar{x} \mathbf{x}', \quad t = \bar{t} t',$$

whereas the velocities (in the two different kinetic equations) scale differently for ions and electrons, namely

$$\mathbf{v}_i = \bar{v}_i \mathbf{v}', \quad \mathbf{v}_e = \bar{v}_e \mathbf{v}'.$$

This different scaling in the velocities is fundamental for the further study, the rescaled velocities \mathbf{v}' being now of the same order for ions and electrons, fact which is a considerable advantage for numerical simulations. Furthermore, in (2.2) we set

$$\mathbf{E}(t, \mathbf{x}) = \bar{E} \mathbf{E}'(t', \mathbf{x}').$$

Altogether one obtains then the following non-dimensional system (the primes were omitted for simplicity reasons)

$$(2.8) \quad \begin{cases} \partial_t f_i + \mathbf{v} \cdot \nabla_{\mathbf{x}} f_i + \mathbf{E} \cdot \nabla_{\mathbf{v}} f_i = \frac{1}{\tau} (\mathcal{Q}_{ii}(f_i, f_i) + \varepsilon \mathcal{Q}_{ie}(f_i, f_e)) , \\ \partial_t f_e + \frac{1}{\varepsilon} \mathbf{v} \cdot \nabla_{\mathbf{x}} f_e - \frac{1}{\varepsilon} \mathbf{E} \cdot \nabla_{\mathbf{v}} f_e = \frac{1}{\tau \varepsilon} (\mathcal{Q}_{ee}(f_e, f_e) + \mathcal{Q}_{ei}(f_e, f_i)) , \end{cases}$$

supplemented with Poisson's equation

$$-\lambda^2 \Delta \phi = n_i - n_e, \quad \mathbf{E} = -\nabla_{\mathbf{x}} \phi.$$

Starting from this non-dimensional model, we choose the following regime:

- the ratio between micro and macro time-scales is considered fixed $\tau = 1$;
- the ratio between micro and macro space-scales is considered also fixed $\lambda = 1$;
- the electron-to-ion mass ratio $\varepsilon \ll 1$, will be the only perturbation parameter we shall take into account.

This choice permits to focus on the electron adiabatic asymptotics, without adding additional difficulties coming from the quasi-neutral limit $\lambda \ll 1$ studied for instance in [4, 18]. The fact that we set $\tau = 1$ is justified by our aim to keep the ions kinetic. Other asymptotic regimes can be naturally investigated.

The rescaled macroscopic quantities are given now for $\alpha \in \{e, i\}$ by

$$\begin{cases} n_\alpha := \int_{\mathbb{R}^d} f_\alpha \, d\mathbf{v} , \\ n_\alpha \mathbf{u}_\alpha := \int_{\mathbb{R}^d} \mathbf{v} f_\alpha \, d\mathbf{v} , \\ w_\alpha := \frac{1}{2} \int_{\mathbb{R}^d} |\mathbf{v}|^2 f_\alpha \, d\mathbf{v} = \frac{d}{2} n_\alpha T_\alpha + \frac{1}{2} n_\alpha |\mathbf{u}_\alpha|^2 , \end{cases}$$

where

$$d n_\alpha T_\alpha := \int_{\mathbb{R}^d} |\mathbf{v} - \mathbf{u}_\alpha|^2 f_\alpha \, d\mathbf{v} ,$$

and the pressure tensor \mathbb{P}_α as well as the heat flux \mathbf{q}_α are given by

$$\begin{cases} \mathbb{P}_\alpha := \int_{\mathbb{R}^d} (\mathbf{v} - \mathbf{u}_\alpha) \otimes (\mathbf{v} - \mathbf{u}_\alpha) f_\alpha \, d\mathbf{v} , \\ \mathbf{q}_\alpha := \frac{1}{2} \int_{\mathbb{R}^d} (\mathbf{v} - \mathbf{u}_\alpha) |\mathbf{v} - \mathbf{u}_\alpha|^2 f_\alpha \, d\mathbf{v} , \end{cases}$$

whereas the non-dimensional collision operators read now for $\alpha \in \{e, i\}$ as

$$\mathcal{Q}_{\alpha\alpha}(f_\alpha, f_\alpha) = \nu_{\alpha\alpha} \operatorname{div}_{\mathbf{v}} ((\mathbf{v} - \mathbf{u}_\alpha) f_\alpha + T_\alpha \nabla_{\mathbf{v}} f_\alpha) ,$$

and

$$\begin{cases} \mathcal{Q}_{ei}(f_e, f_i) = \nu_{ei} \operatorname{div}_{\mathbf{v}} ((\mathbf{v} - \mathbf{u}_{ei}) f_e + T_{ei} \nabla_{\mathbf{v}} f_e) , \\ \mathcal{Q}_{ie}(f_i, f_e) = \nu_{ie} \operatorname{div}_{\mathbf{v}} \left((\mathbf{v} - \frac{\mathbf{u}_{ie}}{\varepsilon}) f_i + T_{ie} \nabla_{\mathbf{v}} f_i \right) , \end{cases}$$

with the mixed quantities

$$(2.9) \quad \mathbf{u}_{ei} = \frac{\mathbf{u}_e + \varepsilon \mathbf{u}_i}{2} = \mathbf{u}_{ie} ,$$

$$(2.10) \quad T_{ei} = T_{ie} = \frac{1}{1 + \varepsilon^2} \left(T_e + \varepsilon^2 T_i + \frac{|\mathbf{u}_e - \varepsilon \mathbf{u}_i|^2}{2d} \right).$$

To give only an example for these scalings, let us detail the temperature rescaling. Starting from (2.6) and using the characteristic values defined in Section 2.2 one obtains

$$T_{ei} = \bar{T} \frac{T'_e + m_e/m_i T'_i}{m_e/m_i + 1} + \frac{m_e \bar{u}_e^2}{1 + m_e/m_i} \frac{|u'_e - \frac{\bar{u}_i}{\bar{u}_e} u'_i|^2}{2dk_B} = \frac{\bar{T}}{1 + \varepsilon^2} \left(T'_e + \varepsilon^2 T'_i + \frac{|u'_e - \varepsilon \mathbf{u}'_i|^2}{2d} \right).$$

The non-dimensional model (2.8)-(2.10) will be our starting point for the $\varepsilon \rightarrow 0$ asymptotic study. One can observe that the time scale of interest in this paper corresponds to the average time between two ionic collisions. This time is much larger than the characteristic time of electron collisions. As a consequence, we can expect that in the limit $\varepsilon \rightarrow 0$ the ions remain kinetic and the electrons reach a certain macroscopic regime due to the numerous collisions they undertake.

Let us now prove the properties of conservation and entropy decay, already presented for the dimensional operators. Firstly, let us introduce for $\alpha \in \{e, i\}$ the adimensional Maxwellian distributions \mathcal{M}_α obtained by rescaling (2.3), *i.e.*

$$\mathcal{M}_\alpha(t, x, v) := \frac{n_\alpha}{(2\pi T_\alpha)^{d/2}} \exp\left(-\frac{|\mathbf{v} - \mathbf{u}_\alpha|^2}{2T_\alpha}\right), \quad \forall \alpha \in \{e, i\},$$

which correspond to the equilibrium distributions of the operators \mathcal{Q}_{ee} and \mathcal{Q}_{ii} . Then we also define the equilibria for \mathcal{Q}_{ei} and \mathcal{Q}_{ie} via

$$\begin{cases} \mathcal{M}_{ei}(t, x, v) := \frac{n_e}{(2\pi T_{ei})^{d/2}} \exp\left(-\frac{|\mathbf{v} - \mathbf{u}_{ei}|^2}{2T_{ei}}\right), \\ \mathcal{M}_{ie}(t, x, v) := \frac{n_i}{(2\pi T_{ie})^{d/2}} \exp\left(-\frac{|\varepsilon \mathbf{v} - \mathbf{u}_{ie}|^2}{2\varepsilon^2 T_{ie}}\right), \end{cases}$$

which are nothing but the rescaled versions of (2.7). To simplify the formulae, let us denote in the following by $h_{\alpha\beta}$ respectively h_α the functions

$$(2.11) \quad h_{\alpha\beta} := \frac{f_\alpha}{\mathcal{M}_{\alpha\beta}}, \quad h_\alpha := h_{\alpha\alpha}.$$

With these new notations, we can rewrite the collision operators in the simpler form

$$\mathcal{Q}_{\alpha\beta}(f_\alpha, f_\beta) = \nu_{\alpha\beta} \operatorname{div}_{\mathbf{v}}(T_{\alpha\beta} \mathcal{M}_{\alpha\beta} \nabla_{\mathbf{v}} h_{\alpha\beta}), \quad \forall \alpha, \beta \in \{e, i\}.$$

Proposition 2.1. *Under the constraint*

$$(2.12) \quad \nu_{ei} n_e = \nu_{ie} n_i,$$

corresponding to the rescaled version of (2.4), we have the following conservations

$$\int_{\mathbb{R}^d} \mathcal{Q}_{ei}(f_e, f_i) \begin{pmatrix} \mathbf{v} \\ |\mathbf{v}|^2 \\ 2 \end{pmatrix} d\mathbf{v} + \int_{\mathbb{R}^d} \mathcal{Q}_{ie}(f_i, f_e) \begin{pmatrix} \varepsilon \mathbf{v} \\ \varepsilon^2 |\mathbf{v}|^2 \\ 2 \end{pmatrix} d\mathbf{v} = 0.$$

Furthermore, defining the inter-species entropy dissipation \mathcal{I} by

$$(2.13) \quad \mathcal{I}(t, x) := - \int_{\mathbb{R}^d} [\mathcal{Q}_{ei}(f_e, f_i) \ln(f_e) + \varepsilon^2 \mathcal{Q}_{ie}(f_i, f_e) \ln(f_i)] d\mathbf{v},$$

we have

$$\mathcal{I} = \int_{\mathbb{R}^d} \left[\nu_{ei} T_{ei} \frac{\mathcal{M}_{ei}}{h_{ei}} |\nabla_v h_{ei}|^2 + \varepsilon^2 \nu_{ie} T_{ie} \frac{\mathcal{M}_{ie}}{h_{ie}} |\nabla_v h_{ie}|^2 \right] dv \geq 0.$$

Proof. Conservations of mass, momentum and energy follow from direct computations, whereas entropy dissipation is obtained observing simply that

$$(2.14) \quad \int_{\mathbb{R}^d} \mathcal{Q}_{ei}(f_e, f_i) \ln(\mathcal{M}_{ei}) d\mathbf{v} + \varepsilon^2 \int_{\mathbb{R}^d} \mathcal{Q}_{ie}(f_i, f_e) \ln(\mathcal{M}_{ie}) d\mathbf{v} = 0.$$

□

For the investigation of the asymptotic limit $\varepsilon \rightarrow 0$ it will be necessary to have in mind the rescaled macroscopic electron equations corresponding to (2.8), namely

$$(2.15) \quad \begin{cases} \varepsilon \partial_t n_e + \operatorname{div}_{\mathbf{x}}(n_e \mathbf{u}_e) = 0, \\ \varepsilon \partial_t(n_e \mathbf{u}_e) + \operatorname{div}_{\mathbf{x}}(n_e \mathbf{u}_e \otimes \mathbf{u}_e + \mathbb{P}_e) + n_e \mathbf{E} = -\nu_{ei} n_e \frac{\mathbf{u}_e - \varepsilon \mathbf{u}_i}{2}, \\ \varepsilon \partial_t w_e + \operatorname{div}_{\mathbf{x}}(w_e \mathbf{u}_e + \mathbb{P}_e \mathbf{u}_e + \mathbf{q}_e) + n_e \mathbf{u}_e \cdot \mathbf{E} = S_{ei}, \end{cases}$$

where the energy exchange term reads

$$(2.16) \quad S_{ei} := \int_{\mathbb{R}^d} \mathcal{Q}_{ei}(f_e, f_i) \frac{|\mathbf{v}|^2}{2} d\mathbf{v} = -\nu_{ei} n_e \left[d(T_e - T_{ei}) + \mathbf{u}_e \cdot \frac{\mathbf{u}_e - \varepsilon \mathbf{u}_i}{2} \right],$$

consisting of a first term corresponding to the temperature equilibration and a second term corresponding to the work done by friction. Observe that if we assume that all macroscopic quantities are uniformly bounded with respect to ε , and replacing T_{ei} by the expression (2.10), we obtain

$$S_{ei} = \nu_{ei} n_e \left(-\frac{\varepsilon}{2} \mathbf{u}_i \cdot \mathbf{u}_e + \varepsilon^2 d(T_i - T_e) + \varepsilon^2 \frac{|\mathbf{u}_i|^2 - |\mathbf{u}_e|^2}{2} \right) + \mathcal{O}(\varepsilon^3),$$

which permits to see that temperature equilibration between ions and electrons occurs on a long time scale when ε is small (factor ε^2) which means that ions and electrons can become Maxwellians (due to the collisions) long before their temperature equilibrate. This system is not closed as the pressure tensor \mathbb{P}_e and the heat flux \mathbf{q}_e cannot be expressed with the help of the other three macroscopic variables (n_e, \mathbf{u}_e, w_e) . However in the limit $\varepsilon \rightarrow 0$ one can close this system, as shall be shown in the sequel, the asymptotic model being given in Theorem 3.1.

3. FORMAL DERIVATION OF THE ASYMPTOTIC MODEL

Let us consider from now the one-dimensional case. The main goal of this section is to understand more about the asymptotic limit $\varepsilon \rightarrow 0$ of the following kinetic system

$$(3.1) \quad \begin{cases} \partial_t f_i^\varepsilon + v \partial_x f_i^\varepsilon + E^\varepsilon \partial_v f_i^\varepsilon = \mathcal{Q}_{ii}(f_i^\varepsilon, f_i^\varepsilon) + \varepsilon \mathcal{Q}_{ie}(f_i^\varepsilon, f_e^\varepsilon), \\ \varepsilon \partial_t f_e^\varepsilon + v \partial_x f_e^\varepsilon - E^\varepsilon \partial_v f_e^\varepsilon = \mathcal{Q}_{ee}(f_e^\varepsilon, f_e^\varepsilon) + \mathcal{Q}_{ei}(f_e^\varepsilon, f_i^\varepsilon), \end{cases}$$

coupled to Poisson's equation

$$(3.2) \quad -\partial_{xx} \phi^\varepsilon = n_i^\varepsilon - n_e^\varepsilon, \quad E^\varepsilon = -\partial_x \phi^\varepsilon.$$

To fix the potential, let us impose the constraint of zero average

$$(3.3) \quad \int_{\mathbb{T}} \phi^\varepsilon(t, x) dx = 0, \quad \forall t > 0.$$

The study of the asymptotic $\varepsilon \rightarrow 0$ requires estimates that are uniform with respect to ε . For our coupled system, the only natural identities providing such bounds are mass conservation, free energy and entropy inequalities. Let us first introduce the kinetic energy associated with each species

$$K(t) := K_e(t) + K_i(t),$$

where

$$K_\alpha := \frac{1}{2} \iint_{\mathbb{T} \times \mathbb{R}} |v|^2 f_\alpha^\varepsilon dv dx, \quad \forall \alpha \in \{e, i\}.$$

The characteristic energy related to the electrostatic effects is the electric energy and reads

$$U(t) := \frac{1}{2} \int_{\mathbb{T}} |\partial_x \phi^\varepsilon|^2 dx = \frac{1}{2} \int_{\mathbb{T}} \phi^\varepsilon (n_i^\varepsilon - n_e^\varepsilon) dx,$$

where the last equality stems from Poisson's equation. With these notation we have now the following result.

Proposition 3.1. (Energy conservation) *Suppose that $(f_e^\varepsilon, f_i^\varepsilon, \phi^\varepsilon)$ is a solution of (3.1)-(3.3) such that f_e^ε and f_i^ε are nonnegative and satisfy initially*

$$(3.4) \quad \iint_{\mathbb{T} \times \mathbb{R}} [f_e^\varepsilon(0) + f_i^\varepsilon(0)] (1 + |v|^2) dv dx < \infty.$$

Then, one has the energy conservation, for all $\varepsilon > 0$

$$\mathcal{E}(t) := U(t) + K(t) = \mathfrak{E}, \quad \forall t \geq 0,$$

where \mathfrak{E} is given by the initial value

$$(3.5) \quad \mathfrak{E} := \mathcal{E}(0) < \infty.$$

Proof. Let us first remark that the condition (3.4) together with (3.2) implies $\|\partial_x \phi^\varepsilon(0)\|_{L^2(\mathbb{T})}^2 < \infty$, such that we have indeed a bounded initial energy $\mathcal{E}(0) < \infty$.

Now, let us multiply the first equation in (3.1) by $\varepsilon v^2/2$, the second one by $v^2/2$ and integrate with respect to $(x, v) \in \mathbb{T} \times \mathbb{R}$. This yields after summing up the two equations and integrating by parts

$$(3.6) \quad \begin{aligned} & \varepsilon \frac{dK}{dt}(t) - \int_{\mathbb{T}} E^\varepsilon (\varepsilon n_i^\varepsilon u_i^\varepsilon - n_e^\varepsilon u_e^\varepsilon) dx \\ &= \frac{1}{2} \iint_{\mathbb{T} \times \mathbb{R}} |v|^2 (\varepsilon^2 \mathcal{Q}_{ie}(f_i^\varepsilon, f_e^\varepsilon) + \mathcal{Q}_{ei}(f_e^\varepsilon, f_i^\varepsilon)) dv dx. \end{aligned}$$

On one hand, applying Proposition 2.1, we show that the right hand side vanishes. On the other hand from the continuity equation

$$\varepsilon \partial_t (n_i^\varepsilon - n_e^\varepsilon) + \partial_x (\varepsilon n_i^\varepsilon u_i^\varepsilon - n_e^\varepsilon u_e^\varepsilon) = 0,$$

and Poisson's equation for ϕ^ε , we get that the second term in (3.6) becomes

$$- \int_{\mathbb{T}} E^\varepsilon (\varepsilon n_i^\varepsilon u_i^\varepsilon - n_e^\varepsilon u_e^\varepsilon) dx = \varepsilon \frac{dU}{dt}(t).$$

Finally gathering the latter equalities, we get the conservation of the total energy

$$\varepsilon \frac{d\mathcal{E}}{dt}(t) = \varepsilon \frac{d}{dt} (U(t) + K(t)) = 0, \quad \forall t \geq 0.$$

□

Let us define now the entropy of each species by the formula

$$\mathcal{H}_\alpha(t) := \iint_{\mathbb{T} \times \mathbb{R}} f_\alpha^\varepsilon \ln(f_\alpha^\varepsilon) dv dx, \quad \forall \alpha \in \{e, i\},$$

and prove the following result.

Proposition 3.2. (Entropy decay) *Suppose that $(f_e^\varepsilon, f_i^\varepsilon, \phi^\varepsilon)$ is a solution of (3.1)-(3.3), such that f_e^ε and f_i^ε are nonnegative, satisfying moreover*

$$(3.7) \quad \mathcal{H}_e(0) + \mathcal{H}_i(0) < \infty.$$

Then, one has the following entropy estimate, for all $\varepsilon > 0$

$$\begin{aligned} \mathcal{H}_e(t) + \mathcal{H}_i(t) &+ \frac{1}{\varepsilon} \int_0^t \iint_{\mathbb{T} \times \mathbb{R}} \left[\nu_{ee} T_{ee}^\varepsilon \frac{\mathcal{M}_e}{h_e^\varepsilon} |\partial_v h_e^\varepsilon|^2 + \nu_{ei} T_{ei}^\varepsilon \frac{\mathcal{M}_{ei}}{h_{ei}^\varepsilon} |\partial_v h_{ei}^\varepsilon|^2 \right] dv dx ds \\ &+ \int_0^t \iint_{\mathbb{T} \times \mathbb{R}} \left[\nu_{ii} T_{ii}^\varepsilon \frac{\mathcal{M}_i}{h_i^\varepsilon} |\partial_v h_i^\varepsilon|^2 + \varepsilon \nu_{ie} T_{ie}^\varepsilon \frac{\mathcal{M}_{ie}}{h_{ie}^\varepsilon} |\partial_v h_{ie}^\varepsilon|^2 \right] dv dx ds \\ &\leq \mathcal{H}_e(0) + \mathcal{H}_i(0), \quad \forall t \geq 0, \end{aligned}$$

where h_{ei}^ε and h_{ie}^ε are given in (2.11).

Proof. The entropy estimates are obtained by multiplying the first two equations of (3.1) by $\varepsilon(\ln(f_i^\varepsilon) + 1)$ and $\ln(f_e^\varepsilon) + 1$ respectively and integrating in (x, v) . This yields

$$\begin{aligned} \varepsilon \frac{d}{dt} (\mathcal{H}_e(t) + \mathcal{H}_i(t)) &= -\nu_{ee} \iint_{\mathbb{T} \times \mathbb{R}} T_{ee}^\varepsilon \frac{\mathcal{M}_e}{h_e^\varepsilon} |\partial_v h_e^\varepsilon|^2 dv dx \\ &\quad - \varepsilon \nu_{ii} \iint_{\mathbb{T} \times \mathbb{R}} T_{ii}^\varepsilon \frac{\mathcal{M}_i}{h_i^\varepsilon} |\partial_v h_i^\varepsilon|^2 dv dx - \int_{\mathbb{T}} \mathcal{I}(t, x) dx, \end{aligned}$$

where \mathcal{I} is given in (2.13). For these computations we needed again (2.14) as well as the conservation laws. Dividing by ε and using the expression of \mathcal{I} , permits to get

$$\begin{aligned} \frac{d}{dt} (\mathcal{H}_e(t) + \mathcal{H}_i(t)) &= -\frac{1}{\varepsilon} \iint_{\mathbb{T} \times \mathbb{R}} \left[\nu_{ee} T_{ee}^\varepsilon \frac{\mathcal{M}_e}{h_e^\varepsilon} |\partial_v h_e^\varepsilon|^2 + \nu_{ei} T_{ei}^\varepsilon \frac{\mathcal{M}_{ei}}{h_{ei}^\varepsilon} |\partial_v h_{ei}^\varepsilon|^2 \right] dv dx \\ &\quad - \iint_{\mathbb{T} \times \mathbb{R}} \left[\nu_{ii} T_{ii}^\varepsilon \frac{\mathcal{M}_i}{h_i^\varepsilon} |\partial_v h_i^\varepsilon|^2 + \varepsilon \nu_{ie} T_{ie}^\varepsilon \frac{\mathcal{M}_{ie}}{h_{ie}^\varepsilon} |\partial_v h_{ie}^\varepsilon|^2 \right] dv dx. \end{aligned}$$

Integrating over $[0, t]$ and keeping only the two dominant terms on the right hand side, yields the entropy estimate with the corresponding dissipation. \square

Now, let us formally derive the asymptotic model when $\varepsilon \rightarrow 0$.

Theorem 3.1. (Asymptotic limit) *Suppose that for each $\varepsilon > 0$, $(f_e^\varepsilon, f_i^\varepsilon, \phi^\varepsilon)$ is a solution to the coupled system (3.1)-(3.3) satisfying (2.12), (3.4)-(3.5), (3.7) and*

$$\iint_{\mathbb{T} \times \mathbb{R}} f_e^\varepsilon(t=0, x, v) dv dx = \iint_{\mathbb{T} \times \mathbb{R}} f_i^\varepsilon(t=0, x, v) dv dx = \mathfrak{N},$$

for some fixed $\mathfrak{N} > 0$. Furthermore, for any final time $T_{\text{end}} > 0$, let us assume that the family defined by the macroscopic quantities $\mathbf{U}_\alpha^\varepsilon = (n_\alpha^\varepsilon, u_\alpha^\varepsilon, T_\alpha^\varepsilon)$ for $\alpha \in \{e, i\}$ are relatively compact

in $L^1(0, T_{\text{end}}, L^\infty(\mathbb{T}))$. Then, when ε tends towards zero, the distribution function f_e^ε tends towards a local Maxwellian f_e^0 of the form (Maxwell-Boltzmann distribution)

$$(3.8) \quad \begin{cases} f_e^0(t, x, v) = \frac{n_e^0(t, x)}{\sqrt{2\pi T_e^0(t)}} \exp\left(-\frac{v^2}{2T_e^0(t)}\right), \\ n_e^0(t, x) = c^0(t) \exp\left(\frac{\phi^0(t, x)}{T_e^0(t)}\right), \end{cases}$$

where $c^0(t)$ is given such that

$$(3.9) \quad \int_{\mathbb{T}} n_e^0(t, x) dx = \mathfrak{N}, \quad \forall t \geq 0,$$

whereas (ϕ^0, T_e^0) is such that $T_e^0(t)$ only depends on the time-variable, and is computed via the energy conservation

$$(3.10) \quad \frac{\mathfrak{N}}{2} T_e^0(t) + \frac{1}{2} \int_{\mathbb{T}} |\partial_x \phi^0(t, x)|^2 dx + \frac{1}{2} \iint_{\mathbb{T} \times \mathbb{R}} f_i^0(t, x, v) v^2 dv dx = \mathfrak{E}, \quad \forall t \geq 0$$

and ϕ^0 is solution to the nonlinear Poisson-Boltzmann equation

$$(3.11) \quad -\partial_{xx} \phi^0 + c^0(t) \exp\left(\frac{\phi^0}{T_e^0(t)}\right) = n_i^0, \quad E^0 = -\partial_x \phi^0,$$

supplied with the additional constraint

$$(3.12) \quad \int_{\mathbb{T}} \phi^0(t, x) dx = 0, \quad \forall t \geq 0.$$

The ion distribution function f_i^0 satisfies then the Vlasov-Fokker-Planck equation

$$(3.13) \quad \begin{cases} \partial_t f_i^0 + v \partial_x f_i^0 + E^0 \partial_v f_i^0 = \mathcal{Q}_{ii}(f_i^0, f_i^0), \\ n_i^0 = \int_{\mathbb{R}} f_i^0 dv. \end{cases}$$

Proof. On one hand, thanks to the uniform bounds established in Proposition 3.1 and 3.2 on the total energy and the entropy, one can show that up to a subsequence we have for $\alpha \in \{e, i\}$

$$f_\alpha^\varepsilon \rightharpoonup f_\alpha^0 \quad \text{weakly-}\star \text{ in } L^\infty(0, T_{\text{end}}, L^1(\mathbb{T} \times \mathbb{R})), \quad \text{as } \varepsilon \rightarrow 0.$$

On the other hand, from the assumption on the densities n_e^ε and n_i^ε and using Poisson's equation (3.2), we can show that up to a subsequence, E^ε converges to E^0 strongly in $L^1(0, T_{\text{end}}, L^\infty(\mathbb{T}))$. Together with the weak-* convergence of the distribution function $(f_i^\varepsilon)_{\varepsilon>0}$ and $(f_e^\varepsilon)_{\varepsilon>0}$ in $L^\infty(0, T_{\text{end}}, L^1(\mathbb{T} \times \mathbb{R}))$, this yields for $\alpha \in \{i, e\}$, and for any test function $\varphi \in \mathcal{C}_c^\infty([0, T_{\text{end}}] \times \mathbb{T} \times \mathbb{R})$,

$$\int_0^{T_{\text{end}}} \iint_{\mathbb{T} \times \mathbb{R}} E^\varepsilon f_\alpha^\varepsilon \partial_v \varphi dx dv dt \rightarrow \int_0^{T_{\text{end}}} \iint_{\mathbb{T} \times \mathbb{R}} E^0 f_\alpha^0 \partial_v \varphi dx dv dt, \quad \text{as } \varepsilon \rightarrow 0.$$

Furthermore, using that $(n_\alpha^\varepsilon, u_\alpha^\varepsilon, T_\alpha^\varepsilon)_{\varepsilon>0}$ is relatively compact in $L^1(0, T_{\text{end}}, L^\infty(\mathbb{T}))$, we also get that $\mathcal{Q}_{\alpha\beta}(f_\alpha^\varepsilon, f_\beta^\varepsilon)$ weakly converges to $\mathcal{Q}_{\alpha\beta}(f_\alpha^0, f_\beta^0)$. Altogether we have thus that the limit (f_e^0, f_i^0) is a solution to the following system

$$(3.14) \quad \begin{cases} \partial_t f_i^0 + v \partial_x f_i^0 + E^0 \partial_v f_i^0 = \mathcal{Q}_{ii}(f_i^0, f_i^0) - \nu_{ie} \frac{u_e^0}{2} \partial_v f_i^0, \\ v \partial_x f_e^0 - E^0 \partial_v f_e^0 = \mathcal{Q}_{ee}(f_e^0, f_e^0) + \mathcal{Q}_{ei}(f_e^0, f_i^0), \end{cases}$$

coupled with Poisson's equation for the potential ϕ^0

$$-\partial_{xx}\phi^0 = n_i^0 - n_e^0, \quad E^0 = -\partial_x\phi^0,$$

with the constraint of zero average

$$\int_{\mathbb{T}} \phi^0(t, x) dx = 0, \quad \forall t > 0.$$

It remains to check that in the $\varepsilon \rightarrow 0$ limit $u_e^0 = 0$ and f_e^0 is of the form of a local Maxwellian. Indeed, in view of the entropy dissipation given in Proposition 3.2 and the conservation of mass, we obtain

$$f_e^0 = \mathcal{M}_{n_e^0, u_e^0, T_e^0} \quad \text{and} \quad f_e^0 = \mathcal{M}_{n_e^0, u_{ei}^0, T_{ei}^0},$$

where $u_{ei}^0 = u_e^0/2$ and $T_{ei}^0 = T_e^0 + |u_e^0|^2/2$ are obtained by passing to the limit in (2.9)-(2.10). Hence this yields that $u_e^0 = 0$ and that f_e^0 is a local Maxwellian of the form

$$f_e^0(t, x, v) = \mathcal{M}_{n_e^0, 0, T_e^0},$$

whereas the unknowns (n_e^0, T_e^0) are still to be determined. Finally, inserting now the Maxwellian $f_e^0 = \mathcal{M}_{n_e^0, 0, T_e^0}$ in the second equation of (3.14), yields

$$v \partial_x \mathcal{M}_{n_e^0, 0, T_e^0} - E^0 \partial_v \mathcal{M}_{n_e^0, 0, T_e^0} = 0,$$

or equivalently

$$v \left[\frac{\partial_x n_e^0}{n_e^0} + \left(\frac{v^2}{2T_e^0} - \frac{1}{2} \right) \frac{\partial_x T_e^0}{T_e^0} \right] - v \frac{\partial_x \phi^0}{T_e^0} = 0.$$

This permits to get the asymptotic model (3.8)-(3.13), by comparing the terms of the same order in v . \square

It is for the moment not clear if it is possible to perform this formal proof even at the fluid level, meaning starting from the electron moment equations (2.15). It seems that only the kinetic framework, especially the powerful H-theorem, permits to obtain that in the limit the mean electron velocity vanishes $u_e \equiv 0$ and that the temperature $T_e^0(t)$ is only time-dependent.

Remark 3.1. *The Limit-model (3.8)-(3.13) has an equivalent formulation given by*

$$(3.15) \quad (L)' \left\{ \begin{array}{l} \partial_t f_i^0 + v \partial_x f_i^0 + E^0 \partial_v f_i^0 = \nu_{ii} \partial_v [(v - u_i^0) f_i^0 + T_i^0 \partial_v f_i^0], \\ v \partial_x f_e^0 - E^0 \partial_v f_e^0 = (\nu_{ee} + \nu_{ei}) \partial_v [v f_e^0 + T_e^0 \partial_v f_e^0], \\ -\partial_{xx}\phi^0 = n_i^0 - n_e^0, \quad E^0 = -\partial_x\phi^0, \\ \int_{\mathbb{T}} n_e^0(t, x) dx = \int_{\mathbb{T}} n_i^0(t, x) dx = \mathfrak{N}, \quad \forall t \geq 0, \\ \frac{1}{2} \iint_{\mathbb{T} \times \mathbb{R}} f_e^0(t, x, v) v^2 dv dx + \frac{1}{2} \int_{\mathbb{T}} |\partial_x \phi^0(t, x)|^2 dx + \frac{1}{2} \iint_{\mathbb{T} \times \mathbb{R}} f_i^0(t, x, v) v^2 dv dx = \mathfrak{E}. \end{array} \right.$$

The next theorem certifies the existence and uniqueness of a solution of the just obtained asymptotic model (3.8)-(3.13), for a given ion distribution function f_i^0 .

Theorem 3.2. (Well posedness of the asymptotic model) *Let us fix the total number of electrons $\mathfrak{N} > 0$ and the initial energy $\mathfrak{E} > 0$. Furthermore, assume that the ion distribution function f_i is known, sufficiently smooth and such that $(n_i, w_i) \in L^\infty(\mathbb{R}^+; L^1(\mathbb{T}; \mathbb{R}^+))^2$, satisfying*

$$\int_{\mathbb{T}} n_i dx = \mathfrak{N}.$$

Then there exists a unique solution $(\phi, T_e) \in L^\infty(\mathbb{R}^+; H^1(\mathbb{T})) \times L^\infty(\mathbb{R}^+)$ to the non-linear elliptic problem (3.9)-(3.12). Moreover, if $n_i \in L^\infty(\mathbb{R}^+; L^2(\mathbb{T}))$ one gets $\phi \in L^\infty(\mathbb{R}^+; H^2(\mathbb{T}))$.

Proof. Let us first introduce the space

$$\mathcal{H} := \{ g \in H^1(\mathbb{T}) / \int_{\mathbb{T}} g(x) dx = 0 \}.$$

Observe that in the limit problem (3.9)-(3.12), the time $t \in \mathbb{R}^+$ is simply a parameter, hence we fix and drop it in the sequel. The proof of this theorem is based on the construction and study of the map $\mathcal{E} : \mathbb{R}^+ \rightarrow \mathbb{R}^+$, given for any $T \in \mathbb{R}^+$ by

$$\mathcal{E}(T) := \frac{\mathfrak{N}}{2} T + \frac{1}{2} \int_{\mathbb{T}} |\partial_x \phi_T(t, \cdot)|^2 dx + \int_{\mathbb{T}} w_i(t, \cdot) dx,$$

where ϕ_T is the solution to non-linear elliptic equation (3.11) with conditions (3.9) and (3.12), and with $T_e \equiv T > 0$.

The aim is now to show that there exists $T_\star > 0$ such that $\mathcal{E}(T_\star) = \mathfrak{E}$. This shall be done in several steps: first we prove that for any $T > 0$ there exists a smooth potential, denoted ϕ_T , to (3.11) with conditions (3.9) and (3.12), hence that $\mathcal{E}(T)$ is a well-defined mapping; secondly we shall prove that this mapping \mathcal{E} is continuous, nondecreasing with $\mathcal{E}(0) \leq \mathfrak{E}$ and

$$\lim_{T \rightarrow \infty} \mathcal{E}(T) = \infty.$$

Step 1 : Study of the map $T > 0 \mapsto \phi_T \in \mathcal{H}$ for fixed $t \in \mathbb{R}^+$. For a given $T > 0$ standard elliptic theory permits to show the existence and uniqueness of a solution $\phi_T \in \mathcal{H}$ to the non-linear elliptic equation (3.11) with conditions (3.9) and (3.12). This is based on the minimization of the strictly convex, differentiable functional on the space \mathcal{H}

$$\mathcal{L}(\phi) := \frac{1}{2} \int_{\mathbb{T}} |\partial_x \phi|^2 dx + \mathfrak{N} T \ln \left(\int_{\mathbb{T}} e^{\phi/T} dx \right) - \int_{\mathbb{T}} n_i \phi dx.$$

Remark that one has the compact injection $H^1(\mathbb{T}) \subset C(\overline{\mathbb{T}})$, such that all terms in this expression are well-defined.

To get some estimates on ϕ_T , let us multiply the second equation of (3.11) by ϕ_T and integrate in space, to obtain

$$\begin{aligned} \|\partial_x \phi_T\|_{L^2(\mathbb{T})}^2 &= \int_{\mathbb{T}} n_i \phi_T dx - c(t) \int_{\mathbb{T}} e^{\phi_T/T} \phi_T dx \\ &\leq \mathfrak{N} \|\phi_T\|_{L^\infty(\mathbb{T})} + \mathfrak{N} \|\phi_T\|_{L^\infty(\mathbb{T})} \\ &\leq C \|\phi_T\|_{H^1(\mathbb{T})}, \end{aligned}$$

such that via Poincaré's inequality one gets that ϕ_T is bounded in $H^1(\mathbb{T})$ independently on T .

Step 2 : Study of the map $T \mapsto \mathcal{E}(T)$ for fixed $t \in \mathbb{R}^+$. To continue the proof, it will be simpler to introduce in this step the auxiliary unknown $\psi \in H^1(\mathbb{T})$, solution of the problem

$$(3.16) \quad \begin{cases} -\partial_{xx}\psi + \mathfrak{N}e^{\psi/T} = n_i, \\ \frac{\mathfrak{N}}{2}T + \frac{1}{2} \int_{\mathbb{T}} |\partial_x \psi|^2 dx + \int_{\mathbb{T}} w_i dx = \mathfrak{E}, \end{cases}$$

associated with periodic boundary conditions and the different constraint

$$(3.17) \quad \int_{\mathbb{T}} e^{\psi/T} dx = 1,$$

and to remark that both problems (3.9)-(3.12) and (3.16)-(3.17) are completely equivalent. More precisely, we have the following relation $\psi = \phi + K_T$ with

$$K_T := -T \ln \left(\int_{\mathbb{T}} e^{\phi/T} dx \right),$$

respectively $\phi = \psi + C_T$ with

$$C_T := - \int_{\mathbb{T}} \psi dx,$$

permitting to pass from one problem to the other.

Let us observe that the introduction of the auxiliary unknown ψ_T does not change the map $\mathcal{E}(T)$ which writes now

$$(3.18) \quad \mathcal{E} : \begin{array}{ccc} \mathbb{R}^+ & \mapsto & \mathbb{R}^+ \\ T & \rightarrow & \frac{\mathfrak{N}}{2}T + \frac{1}{2} \int_{\mathbb{T}} |\partial_x \psi_T|^2 dx + \int_{\mathbb{T}} w_i dx. \end{array}$$

One can show that this application is strictly increasing and continuous in T , and that

$$\mathcal{E}(T) \xrightarrow{T \rightarrow \infty} \infty, \quad \mathcal{E}(T) \xrightarrow{T \rightarrow 0} \int_{\mathbb{T}} w_i dx \leq \mathfrak{E}.$$

The $T \rightarrow \infty$ limit is obvious from (3.18). The continuity of \mathcal{E} is based on the continuity of the map $T \mapsto \psi_T \in H^1(\mathbb{T})$. To show this, we fix $T > 0$ and hence $\psi_T \in H^1(\mathbb{T})$ and consider the linear problem

$$(3.19) \quad -\partial_{xx}\theta + \frac{\mathfrak{N}}{T} e^{\psi_T/T} \theta = \frac{\mathfrak{N}}{T^2} e^{\psi_T/T} \psi_T,$$

associated with periodic boundary conditions, problem which admits a unique solution $\theta \in H^2(\mathbb{T})$. Now, one observes that differentiating (in the distributional sense) the first equation in (3.16) with respect to T yields

$$(3.20) \quad -\partial_{xx}(\partial_T \psi_T) = \mathfrak{N} e^{\frac{\psi_T}{T}} \left(\frac{\psi_T}{T^2} - \partial_T \psi_T / T \right),$$

which is nothing but problem (3.19). By uniqueness one has then the existence of $\partial_T \psi_T \in H^2(\mathbb{T})$.

The continuity and monotonicity of \mathcal{E} is shown by computing its derivative with respect to T , namely

$$\frac{d}{dT} \mathcal{E}(T) = \frac{\mathfrak{N}}{2} + \int_{\mathbb{T}} \partial_x \psi_T \partial_{xT} \psi_T dx = \frac{\mathfrak{N}}{2} - \int_{\mathbb{T}} \psi_T \partial_{xx}(\partial_T \psi_T) dx.$$

Inserting in this last formula ψ_T obtained from (3.20), yields

$$\frac{d}{dT}\mathcal{E}(T) = \frac{\mathfrak{N}}{2} + \frac{T^2}{\mathfrak{N}} \int_{\mathbb{T}} e^{-\psi_T/T} |\partial_{xx}(\partial_T \psi_T)|^2 dx + T \int_{\mathbb{T}} |\partial_{xT} \psi_T|^2 dx \geq 0.$$

Finally, to show the limit in $T = 0$ we shall investigate in more details the dependence of ψ_T on T . For this, multiplying the equation (3.16) with ψ and integrating in space, yields

$$\|\partial_x \psi\|_{L^2(\mathbb{T})}^2 + \mathfrak{N} \int_{\mathbb{T}} e^{\psi/T} \psi dx = \int_{\mathbb{T}} n_i \psi dx,$$

thus

$$\begin{aligned} \|\partial_x \psi\|_{L^2(\mathbb{T})}^2 &= \int_{\mathbb{T}} n_i \psi dx - \mathfrak{N} T \int_{\psi \geq 0} e^{\psi/T} \frac{\psi}{T} dx - \mathfrak{N} T \int_{\psi < 0} e^{\psi/T} \frac{\psi}{T} dx \\ &\leq \mathfrak{N} \|\psi\|_{L^\infty(\mathbb{T})} - \frac{\mathfrak{N}}{T} \|\psi\|_{L^2(\mathbb{T})}^2 + \mathfrak{N} T e^{-1} |\mathbb{T}|, \end{aligned}$$

where we used the fact that $e^x \geq x$ for positive x , whereas $-x e^x \leq e^{-1}$ for negative x . This implies $\|\partial_x \psi\|_{L^2(\mathbb{T})}^2 \rightarrow_{T \rightarrow 0} 0$, as $\|\psi\|_{H^1(\mathbb{T})} \leq C$ with a constant $C > 0$ independent on T .

Therefore, by applying Rolle's theorem, there exists a unique $T_\star > 0$ such that $\mathcal{E}(T_\star) = \mathfrak{E}$ and a unique associated $\phi_{T_\star} \in \mathcal{H}$, solution to (3.11) with (3.9) and (3.12).

This concludes the proof for fixed $t \in \mathbb{R}^+$ and we shall denote $T(t) := T_\star$. We remark additionally that $\phi_{T_\star} \in W^{2,1}(\mathbb{T})$ and for more regular data, namely for $n_i(t) \in L^2(\mathbb{T})$, one has even $\phi_{T_\star}(t) \in \mathcal{H} \cap H^2(\mathbb{T})$.

Finally, the regularity in time comes now from the fact that t is only a parameter in the second equation of (3.11). Indeed, from the first step, we know that ϕ_T is bounded in $H^1(\mathbb{T})$ independently on T , and the energy conservation in (3.10) yields the boundedness of $T(t)$, concluding the proof. \square

4. NUMERICAL SCHEME

This section is devoted to the first steps towards the construction of a numerical scheme for the Vlasov-Poisson-Fokker-Planck system (3.1)-(3.3) based on a direct discretization in the (x, v) phase-space (Eulerian approach). In the velocity space, we shall make use of a complete, orthonormal Hermite basis to approach the distribution functions [16, 17]. For the space discretization a discrete Galerkin method is applied for both transport and Poisson equations [2, 16, 17]. The use of a Hermite spectral method to discretize the velocity variable is motivated by the fact that this method, if well scaled, is able to reduce drastically the computational costs in situations where a kinetic-fluid transition is investigated, thus in particular when dealing with our adiabatic limit $\varepsilon \rightarrow 0$. As mentioned in the introduction the here presented scheme is only a first step towards a fully performant numerical method we shall present in a forthcoming work [15]. In this section, we focus solely on the introduction of well-designed Hermite basis functions in the velocity space, permitting to gain considerable time in the electron dynamic resolution when $\varepsilon \ll 1$, and this due to the possibility to reduce dynamically the number of Hermite-modes taken into account. The time stiffness is a second problem, which needs special attention and will be dealt with in a second work [15].

4.1. Hermite expansion for the electron system. We shall start by supposing in this subsection that the ion dynamics is known, with smooth macroscopic quantities (n_i, u_i, T_i) ,

and shall present a numerical scheme solely for the resolution of the electron Vlasov-Poisson-Fokker-Planck system

$$(4.1) \quad \begin{cases} \varepsilon \partial_t f + v \partial_x f - E \partial_v f = \mathcal{Q}(f), \\ -\partial_{xx} \phi = n_i - n, \quad E = -\partial_x \phi, \end{cases}$$

with $\mathcal{Q}(f)$ the mixed, non-linear Fokker-Planck operator

$$\mathcal{Q}(f) = \nu_{ee} \partial_v [(v - u) f + T \partial_v f] + \nu_{ei} \partial_v [(v - u_{ei}) f + T_{ei} \partial_v f],$$

where we recall that the mixed velocities and temperatures are defined in (2.9)-(2.10). The key of the Hermite spectral method is to construct suitable basis functions in the velocity variable in order to cope with the electron asymptotic limit $\varepsilon \rightarrow 0$, in such a way that the limit distribution function is represented by only one Hermite function ψ_0 , reducing naturally the complexity of the kinetic equation to the resolution of only one macroscopic equation, namely the limit model.

Before performing the discretization, we recall the standard (probabilistic) Hermite polynomials $\{J_k\}_{k \in \mathbb{N}}$, which form an orthonormal basis in $L^2(\mathcal{M} dv)$, where

$$\mathcal{M}(v) := \frac{1}{\sqrt{2\pi}} e^{-v^2/2},$$

is the classical Maxwellian distribution function in the velocity variable. These polynomials are defined recursively as $J_0 \equiv 1$, $J_1 \equiv v$, then for any $k \geq 1$ by

$$\sqrt{k+1} J_{k+1} = v J_k(v) - \sqrt{k} J_{k-1},$$

and satisfy

$$J'_k(v) = \sqrt{k} J_{k-1}(v), \quad \int_{\mathbb{R}} J_k(v) J_l(v) \mathcal{M} dv = \delta_{kl}, \quad \forall k, l \in \mathbb{N}.$$

For the study of the here considered Fokker-Planck collision-operators, we have to adapt these standard Hermite polynomials and rescale them adequately as

$$\psi_k(v) := \frac{1}{v_{th}} J_k \left(\frac{v}{v_{th}} \right) \mathcal{M} \left(\frac{v}{v_{th}} \right),$$

where v_{th} is a scaling function to be suitably defined in the sequel, such that these Hermite basis functions are well adapted for the investigation of the asymptotic limit $\varepsilon \rightarrow 0$.

To summarize, we shall expand the electron distribution function $f(t, x, v)$ as follows

$$(4.2) \quad f(t, x, v) := \sum_{k=0}^{\infty} \alpha_k(t, x) \psi_k(t, v),$$

where $\{\psi_k(t, \cdot)\}_{k \in \mathbb{N}}$ forms a complete, orthonormal basis of $L^2(\mathcal{M}_{v_{th}}^{-1} dv)$. The crucial feature of these basis functions is that the chosen weight is given by the “limiting” electron Maxwellian

$$(4.3) \quad \mathcal{M}_{v_{th}(t)}(v) := \frac{1}{\sqrt{2\pi} v_{th}(t)} \exp \left(-\frac{v^2}{2v_{th}^2(t)} \right), \quad v_{th}(t) := \sqrt{T(t)},$$

with $T(t)$ the electron temperature given by the asymptotic limit model (3.10)-(3.12).

These Hermite basis functions are defined recursively as $\psi_0(t, v) \equiv \mathcal{M}_{v_{th}(t)}(v)$, $\psi_1(t, v) \equiv v \mathcal{M}_{v_{th}(t)}/v_{th}(t)$ and for $k \geq 1$ by

$$(4.4) \quad \sqrt{k+1} \psi_{k+1}(t, v) = \frac{v}{v_{th}} \psi_k(t, v) - \sqrt{k} \psi_{k-1}(t, v),$$

and satisfy

$$v_{th} \partial_v \psi_k(t, v) = -\sqrt{k+1} \psi_{k+1}(t, v), \quad \int_{\mathbb{R}} \psi_k(t, v) \psi_l(t, v) \mathcal{M}_{v_{th}}^{-1} dv = \delta_{kl}, \quad \forall k, l \in \mathbb{N}.$$

One should be aware that different scalings of the basis functions lead to different expansion series. Based on a priori knowledge on the behaviour of our solution, the scaling is chosen in such a manner to enable the convergence towards the desired equation, in our case towards the limit model as $\varepsilon \rightarrow 0$. Hence it is important to underline here that for the definition of the Hermite basis functions $\{\psi_k(t, \cdot)\}_{k \in \mathbb{N}}$ one should first solve the limit model (3.10)-(3.12) in order to get the scaling factor $v_{th}(t)$.

The coefficients $\{\alpha_k(t, x)\}_{k \in \mathbb{N}}$ in (4.2) are still to be determined, and are given in the following proposition.

Proposition 4.1. *Let (f, ϕ) be the electron distribution function resp. the potential, solution of the system (4.1), and let us consider the decomposition (4.2) in the Hermite basis functions given in (4.3)-(4.4). Then the Hermite coefficients $\{\alpha_k\}_{k \in \mathbb{N}}$ are solutions to the following coupled, nonlinear, infinite PDE-system*

$$(4.5) \quad \begin{cases} \varepsilon \left(\partial_t \alpha_k + \frac{v'_{th}}{v_{th}} \left[k \alpha_k + \sqrt{(k-1)k} \alpha_{k-2} \right] \right) + v_{th} \partial_x \left(\sqrt{k} \alpha_{k-1} + \sqrt{k+1} \alpha_{k+1} \right) \\ + \sqrt{k} \frac{E}{v_{th}} \alpha_{k-1} + \nu_{ee} \left(k \alpha_k - \sqrt{k} \frac{u}{v_{th}} \alpha_{k-1} + \left[1 - \frac{T}{v_{th}^2} \right] \sqrt{(k-1)k} \alpha_{k-2} \right) \\ + \nu_{ei} \left(k \alpha_k - \sqrt{k} \frac{u_{ei}}{v_{th}} \alpha_{k-1} + \left[1 - \frac{T_{ei}}{v_{th}^2} \right] \sqrt{(k-1)k} \alpha_{k-2} \right) = 0, \end{cases}$$

where we set $\alpha_l \equiv 0$ for $l < 0$, whereas the electron momentum nu and temperature T are linked with the first Hermite expansion coefficients via the formulae

$$(4.6) \quad nu = v_{th} \alpha_1, \quad T = v_{th}^2 \left[1 + \sqrt{2} \frac{\alpha_2}{\alpha_0} - \left(\frac{\alpha_1}{\alpha_0} \right)^2 \right].$$

This system is coupled to Poisson's equation

$$(4.7) \quad -\partial_{xx} \phi = n_i - \alpha_0, \quad E = -\partial_x \phi.$$

Proof. Multiplying (4.1) by α_l and taking the scalar-product in $L^2(\mathcal{M}_{v_{th}}^{-1} dv)$, yields immediately the system (4.5). Observing then that $\langle \psi_k \rangle = 0$ for all $k \neq 0$, fact which is obtained recursively from (4.4), one has with (4.2) that

$$n(t, x) = \int_{\mathbb{R}} f(t, x, v) dv = \alpha_0(t, x),$$

leading to the form (4.7) of Poisson's equation.

Finally, the fact that $\{\psi_k(t, \cdot)\}_{k \in \mathbb{N}}$ forms an orthonormal basis in $L^2(\mathcal{M}_{v_{th}}^{-1} dv)$ means that the hierarchy (4.5)-(4.7) is equivalent to (4.1) and admits thus a unique solution $\{\alpha_k(t, x)\}_{k \in \mathbb{N}}$. \square

There are several advantages when using a Hermite spectral method for the discretization of the velocity variable. Firstly the functions $\{\psi_k\}_{k \in \mathbb{N}}$ form a complete, orthonormal basis of $L^2(\mathcal{M}_{v_{th}}^{-1} dv)$ with respect to the Gaussian weights, such that these basis functions seem to be optimal to approach Maxwellian-like distribution functions in the velocity variable. Secondly, the lower-order terms in the expansion (4.2) are related to the low order moments of the distribution function, meaning to the macroscopic quantities like the density, the momentum and the energy, quantities, which are usually of interest. The kinetic features of the problem are retained by considering more modes in the Hermite expansion (4.2). Thus, such a Hermite spectral method permits somehow to make the link between the kinetic and the fluid descriptions, and is particularly well suited for our asymptotic study $\varepsilon \rightarrow 0$.

To be more precise, one can observe that $\langle v \psi_k \rangle = 0$ for all $k \geq 2$ and $\langle v^2 \psi_k \rangle = 0$ for all $k \geq 3$, obtained again recursively from (4.4), such that the electron momentum nu , energy w and temperature T are linked with the first Hermite expansion coefficients via the formulae (4.6). Substituting these expressions in (4.5), the first three equations for $(\alpha_0, \alpha_1, \alpha_2)$ are given by [16, 17].

$$\begin{cases} \varepsilon \partial_t \alpha_0 + v_{th} \partial_x \alpha_1 = 0, \\ \varepsilon \left(\partial_t \alpha_1 + \frac{v'_{th}}{v_{th}} \alpha_1 \right) + v_{th} \partial_x \left(\alpha_0 + \sqrt{2} \alpha_2 \right) + \frac{E}{v_{th}} \alpha_0 = -\frac{\nu_{ei}}{2} \left(\alpha_1 - \varepsilon \frac{u_i}{v_{th}} \alpha_0 \right), \\ \varepsilon \left(\partial_t \alpha_2 + \sqrt{2} \frac{v'_{th}}{v_{th}} \left[\alpha_0 + \sqrt{2} \alpha_2 \right] \right) + v_{th} \partial_x \left(\sqrt{2} \alpha_1 + \sqrt{3} \alpha_3 \right) + \sqrt{2} \frac{E}{v_{th}} \alpha_1 = \tilde{S}_{ei}, \end{cases}$$

with

$$\tilde{S}_{ei} = -\nu_{ei} \alpha_0 \frac{\sqrt{2}}{v_{th}^2} \left[T_e - T_{ei} + u_e \frac{u_e - \varepsilon u_i}{2} \right],$$

which correspond exactly to the first three moment equations (2.15). Taking into account for both species, we recover the conservations of mass, momentum and total energy

$$\begin{cases} \frac{d}{dt} \int_{\mathbb{T}} \alpha_0 dx = 0, \\ \frac{d}{dt} \int_{\mathbb{T}} [\varepsilon v_{th} \alpha_1 + n_i u_i] dx = 0, \\ \frac{d}{dt} \int_{\mathbb{T}} \left[\frac{v_{th}^2}{2} \left(\alpha_0 + \sqrt{2} \alpha_2 \right) + \frac{1}{2} |\partial_x \phi|^2 + w_i \right] dx = 0. \end{cases}$$

These constraints are automatically fulfilled for $\varepsilon > 0$, however in the limit they have to be imposed in order to get uniqueness of the limit model. Taking formally the limit $\varepsilon \rightarrow 0$ in (4.5) we get the following Proposition.

Proposition 4.2. *In the limit $\varepsilon \rightarrow 0$ the Hermite coefficients $\{\alpha_k^\varepsilon(t, x)\}_{k \in \mathbb{N}}$, solutions to the system (4.5)-(4.7), tend towards some coefficients $\{\alpha_k\}_{k \in \mathbb{N}}$, satisfying the following limit*

PDE-system

$$(4.8) \quad \begin{cases} v_{th} \partial_x \left(\sqrt{k} \alpha_{k-1} + \sqrt{k+1} \alpha_{k+1} \right) + \sqrt{k} \frac{E}{v_{th}} \alpha_{k-1} \\ + \nu_{ee} \left(k \alpha_k - \sqrt{k} \frac{\alpha_1}{\alpha_0} \alpha_{k-1} - \left[\sqrt{2} \frac{\alpha_2}{\alpha_0} - \left(\frac{\alpha_1}{\alpha_0} \right)^2 \right] \sqrt{(k-1)k} \alpha_{k-2} \right) \\ + \nu_{ei} \left(k \alpha_k - \sqrt{k} \frac{\alpha_1}{2\alpha_0} \alpha_{k-1} - \left[\sqrt{2} \frac{\alpha_2}{\alpha_0} - \frac{1}{2} \left(\frac{\alpha_1}{\alpha_0} \right)^2 \right] \sqrt{(k-1)k} \alpha_{k-2} \right) = 0, \\ \int_{\mathbb{T}} \alpha_0 dx = \mathfrak{N}, \quad \frac{1}{2} \int_{\mathbb{T}} \left[v_{th}^2 \left(\alpha_0 + \sqrt{2} \alpha_2 \right) + |\partial_x \phi|^2 + 2 w_i \right] dx = \mathfrak{E}, \end{cases}$$

coupled to Poisson's equation

$$(4.9) \quad -\partial_{xx} \phi = n_i - \alpha_0, \quad E = -\partial_x \phi.$$

This system admits a unique solution $\{\alpha_k(t, x)\}_{k \in \mathbb{N}}$, given by $\alpha_k \equiv 0$ for all $k \neq 0$ and for the zeroth order coefficient by the equation

$$v_{th} \partial_x \alpha_0 + \frac{E}{v_{th}} \alpha_0 = 0,$$

with ϕ given by Poisson's equation and $v_{th}(t) = \sqrt{T_e(t)}$ by the energy equation in (3.10).

Proof. We simply observe that (4.8)-(4.9) is nothing else than the electron Maxwell-Boltzmann relation given by the well-posed limit system (3.8)-(3.13), equivalently rewritten in Remark 3.1 under the form (3.1). \square

4.2. Space/time discretization. In the spirit of [2, 16, 17], we consider now a discontinuous Galerkin approximation for the space discretization of the Vlasov-Fokker-Planck equation, written via the Hermite basis functions under the form (4.5).

We first introduce some notation and start with $\{x_{i+\frac{1}{2}}\}_{i=0}^{i=N_x}$, a partition of $\mathbb{T} = (0, L)$, with $x_{\frac{1}{2}} = 0$, $x_{N_x+\frac{1}{2}} = L$. Each element is denoted by $I_i = [x_{i-\frac{1}{2}}, x_{i+\frac{1}{2}}]$ with length h_i and

$$h = \max_i h_i.$$

For any $l \in \mathbb{N}$ we introduce the finite dimensional discrete, piecewise polynomial space

$$(4.10) \quad V_h^l = \{u \in L^2(0, L), \quad u|_{I_i} \in P_l(I_i), \quad \forall i = 0, \dots, N_x\},$$

where the local space $P_l(I)$ denotes the set of polynomials of degree at most l on the interval I . In the here presented simulations we used second order polynomials, *i.e.* $l = 2$. We further define for any $i \in \{0, \dots, N_x\}$, the jump $[u]_{i+\frac{1}{2}}$ and the average $\{u\}_{i+\frac{1}{2}}$ of u at $x_{i+\frac{1}{2}}$ as

$$[u]_{i+\frac{1}{2}} := u(x_{i+\frac{1}{2}}^+) - u(x_{i+\frac{1}{2}}^-) \quad \text{and} \quad \{u\}_{i+\frac{1}{2}} := \frac{1}{2} \left(u(x_{i+\frac{1}{2}}^+) + u(x_{i+\frac{1}{2}}^-) \right),$$

where $u(x^\pm) := \lim_{\Delta x \rightarrow 0^\pm} u(x + \Delta x)$. We also set

$$u_{i+\frac{1}{2}} = u(x_{i+\frac{1}{2}}), \quad u_{i+\frac{1}{2}}^\pm = u(x_{i+\frac{1}{2}}^\pm).$$

The approximate solution of (4.1), obtained using Hermite polynomials in the velocity variable and a discontinuous Galerkin discretization in the space variable, is reconstructed as

$$(4.11) \quad f_h(t, x, v) = \sum_{k=0}^{N_H-1} \alpha_{k,h}(t, x) \psi_k(t, v),$$

where $\{\psi_k\}_k$ are the basis functions defined by (4.4) and the set $\{\alpha_{k,h}\}_k$ is determined by the discontinuous Galerkin method, employed for solving (4.5) and presented in the following. The truncation index $N_H \in \mathbb{N}$ will be adapted, considering the vicinity to the limit model, as explained in Section 4.3. This reduces the computational costs.

On one hand, we look for an approximation $\alpha_{k,h}(t, \cdot) \in V_h^l$, such that for any $\varphi_k \in V_h^l$, we have

$$(4.12) \quad \varepsilon \frac{d}{dt} \int_{I_j} \alpha_{k,h} \varphi_k dx = b_k^j(E_h, \alpha_h, \varphi_k) + a_k^j(g_k, \varphi_k), \quad 0 \leq k \leq N_H - 1,$$

where b_k^j is an approximation of the source terms of (4.5)

$$(4.13) \quad \begin{cases} b_k^j(E_h, \alpha_h, \varphi_k) &= - \int_{I_j} \left[\varepsilon \mathcal{I}_k k(\alpha_h) + \frac{\sqrt{k} E_h}{v_{th}} \alpha_{k-1,h} + \mathcal{Q}_k k(\alpha_h) \right] \varphi_k dx, \\ \mathcal{I}_k k(\alpha_h) &= \frac{v'_{th}}{v_{th}} \left(k \alpha_{k,h} + \sqrt{(k-1)k} \alpha_{k-2,h} \right), \\ \mathcal{Q}_k k(\alpha_h) &= (\nu_{ee} + \nu_{ei}) k \alpha_k^\varepsilon - \sqrt{k} \frac{\nu_{ee} u^\varepsilon + \nu_{ei} u_{ei}^\varepsilon}{v_{th}} \alpha_{k-1}^\varepsilon \\ &\quad + \left(\nu_{ee} \left[1 - \frac{T^\varepsilon}{v_{th}^2} \right] + \nu_{ei} \left[1 - \frac{T_{ei}^\varepsilon}{v_{th}^2} \right] \right) \sqrt{(k-1)k} \alpha_{k-2}^\varepsilon, \end{cases}$$

whereas a_k^j represents the space derivative approximation, defined by

$$(4.14) \quad \begin{cases} a_k^j(g_k, \varphi_k) &= - \int_{I_j} g_k \varphi_k' dx + \hat{g}_{k,j+\frac{1}{2}} \varphi_{k,j+\frac{1}{2}}^- - \hat{g}_{k,j-\frac{1}{2}} \varphi_{k,j-\frac{1}{2}}^+, \\ g_k &= v_{th} \left(\sqrt{k+1} \alpha_{k+1,h} + \sqrt{k} \alpha_{k-1,h} \right). \end{cases}$$

The numerical flux \hat{g}_k in (4.14) is given by

$$(4.15) \quad \hat{g}_k = \frac{1}{2} [g_k^- + g_k^+ - \delta_k (\alpha_{k,h}^+ - \alpha_{k,h}^-)],$$

with the numerical viscosity coefficient defined for $k = 0$ as $\delta_0 = 0$, corresponding to a centered flux, and for $1 \leq k \leq N_H - 1$ we consider the global Lax-Friedrichs flux with $\delta_k = \delta = \sqrt{N_H} / \alpha_{N_H,h}$. The choice of the centered flux in the case $k = 0$ is made to recover the conservation of the semi-discrete total energy.

On the other hand, we search for an approximation of the electric field E_h . To this end, we need to consider the potential function $\phi_h(t, x)$, such that

$$(4.16) \quad \begin{cases} E_h = -\frac{\partial \phi_h}{\partial x}, \\ \frac{\partial E_h}{\partial x} = n_i - \alpha_{0,h}, \end{cases}$$

which is equivalent to the one dimensional Poisson equation

$$-\frac{\partial^2 \phi_h}{\partial x^2} = n_{i,h} - \alpha_{0,h}.$$

Let us discretize (4.16) via a discontinuous Galerkin approximation. For this, we look for a couple $(\phi_h(t, \cdot), E_h(t, \cdot)) \in V_h^l \times V_h^l$, such that for any η and ζ belonging to V_h^k , we have

$$(4.17) \quad \begin{cases} + \int_{I_j} \phi_h \eta' dx - \hat{\phi}_{h,j+\frac{1}{2}} \eta_{j+\frac{1}{2}}^- + \hat{\phi}_{h,j-\frac{1}{2}} \eta_{j-\frac{1}{2}}^+ = \int_{I_j} E_h \eta dx, \\ - \int_{I_j} E_h \zeta' dx + \hat{E}_{h,j+\frac{1}{2}} \zeta_{j+\frac{1}{2}}^- - \hat{E}_{h,j-\frac{1}{2}} \zeta_{j-\frac{1}{2}}^+ = \int_{I_j} (n_{i,h} - \alpha_{0,h}) \zeta dx, \end{cases}$$

where the numerical fluxes $\hat{\phi}_h$ and \hat{E}_h in (4.17) are taken as

$$(4.18) \quad \begin{cases} \hat{\phi}_h = \{\Phi_h\}, \\ \hat{E}_h = \{E_h\} - \beta [\Phi_h], \end{cases}$$

with β being a positive constant, possibly proportional to $1/h$ (see [9] for more details).

Finally, the last free parameter is $v_{th}(t)$. It is chosen such that our numerical discretization captures well the limit $\varepsilon \rightarrow 0$. Therefore, following Proposition 4.2, we choose $v_{th}(t)$ such that the energy conservation is satisfied in the limit $\varepsilon \rightarrow 0$, namely via the equation for $(\bar{\alpha}_0, \bar{\phi})$,

$$(4.19) \quad \frac{1}{2} \int_{\mathbb{T}} [v_{th}^2 \bar{\alpha}_0 + |\partial_x \bar{\phi}|^2 + 2w_i] dx = \mathfrak{E},$$

where $\bar{\phi}$ solves

$$\begin{cases} \bar{\alpha}_0 = \frac{\mathfrak{N}}{\int_{\mathbb{T}} e^{\bar{\phi}/v_{th}} dx} e^{\bar{\phi}/v_{th}}, \\ -\partial_{xx} \bar{\phi} = n_i - \bar{\alpha}_0. \end{cases}$$

This choice will guarantee that in the limit $\varepsilon \rightarrow 0$ the coefficients $\{\alpha_{k,h}^\varepsilon\}_k$ will be consistent with the Maxwell-Boltzmann distribution (3.8).

Concerning the time-discretization, we apply a second-order Crank-Nicolson scheme to the just introduced discontinuous Galerkin method. We denote by $\alpha = (\alpha_0, \dots, \alpha_{N_H-1})$ the solution to (4.12)–(4.15) and by (\cdot, \cdot) the standard L^2 inner-product on the space interval $(0, L)$, namely

$$(\alpha_n, \varphi) := \int_0^L \alpha_n \varphi dx,$$

and let $\Delta t > 0$ be the time step.

Furthermore let $\alpha_h^m = (\alpha_0^m, \dots, \alpha_{N_H-1}^m)$ be the approximation of the solution α at time $t^m = m \Delta t$ for $m \geq 0$, and let us denote, for an arbitrary variable ξ

$$\xi^{m+1/2} := \frac{1}{2} (\xi^m + \xi^{m+1}).$$

Assuming known α_h^m , we compute now α_h^{m+1} for $k = 0, \dots, N_H - 1$ via

$$(4.20) \quad \frac{(\alpha_k^{m+1} - \alpha_k^m, \varphi_k)}{\Delta t} + a_k(g_k^{m+1/2}, \varphi_k) + b_k(v_{th}^{m+1/2}, \alpha_h^{m+1/2}, E^{m+1/2}, \varphi_k) = 0, \quad \forall \varphi_k \in V_h^l,$$

and solve the DG approximation of the Poisson equation (4.17)–(4.18) to obtain E^{m+1} .

It is worth to emphasize that this time discretization is not necessarily uniformly stable with respect to ε , h and N_H . For an explicit scheme the CFL condition for the system (4.12)–(4.18) would be

$$\Delta t = \mathcal{O}\left(\frac{\varepsilon h}{\sqrt{N_H}}\right),$$

where N_H denotes the number of Hermite coefficients taken into account. Here an iterative solver is applied to solve this nonlinear and ill-conditioned system. In practice, to ensure the convergence of the iterative method, the time-step Δt is still dependent on ε and (h, N_H) . An AP-scheme is further needed to cope with this problem and this requires a further study [15]. However the Crank-Nicolson scheme is well adapted to our approach where the preservation of energy plays a key role.

4.3. Adaptive algorithm for Hermite coefficients. In this subsection, we provide a simple and efficient way to reduce the computational complexity. Indeed, due to the choice of the scaling function v_{th} , we expect that when the solution of the kinetic equation approaches a hydrodynamical regime, the higher order Hermite coefficients will rapidly converge to zero and can then be neglected. Therefore we propose a simple adaptive algorithm at each time iteration to remove small coefficients (see Algorithm 1). Briefly speaking, a Hermite coefficient can be neglected when this coefficient and its neighbours are small. Otherwise, it should be considered. This adaptive procedure allows to remove or to add Hermite coefficients dynamically. As a consequence, the computational complexity will be considerably reduced in the asymptotic regime $\varepsilon \rightarrow 0$ even when the initial datum is not well prepared. Indeed, the initial time layer will be described correctly using a large number of Hermite coefficients, while when the solution approaches the equilibrium fewer and fewer coefficients will be used.

```

for  $k = 3, \dots$  do
  if  $\|\alpha_k^m\|_\infty, \|\alpha_{k+1}^m\|_\infty, \|\alpha_{k-1}^m\|_\infty \leq 10^{-6}$  then
    | set  $I_k^m = 0$  ▷ Contribution of  $\alpha_k^m$  will be neglected
  else
    | set  $I_k^m = 1$  ▷ Contribution of  $\alpha_k^m$  will be considered
  end
end

```

end
Solve the system (4.12)–(4.15) only for $(\alpha_k^{m+1})_k$ such that $I_k^m = 1$, whereas we set $\alpha_k^{m+1} = 0$ for $I_k^m = 0$.

Algorithm 1: Adaptive algorithm for the computation of the Hermite coefficients at time step t^{m+1} , supposing everything known at time step t^m .

5. NUMERICAL SIMULATIONS

In this section we shall present numerical simulations based on the scheme proposed above to investigate in more details the adiabatic regime when $\varepsilon \ll 1$ for the Vlasov-Poisson Fokker-Planck system (4.1). Our aim is to focus on weakly collisional plasmas, where collective effects, due to the transport part, dominate collisional effects. In this situation, we illustrate what happens in this $\varepsilon \rightarrow 0$ adiabatic asymptotic, and in particular we are interested in investigating what is the advantage of using a Hermite spectral-method in the velocity variable, for physically relevant mass ratio $\varepsilon^2 = m_e/m_i$.

5.1. One species case. In this first example, we examine only the electron evolution, the ions being considered as forming a sort of fixed background, interacting with the electrons only via the electric field. Since in this case, the limit $\varepsilon \rightarrow 0$ corresponds to the asymptotic limit $t \rightarrow \infty$, we fix ε to one and investigate the long time behavior of the following equation

$$\begin{cases} \partial_t f + v \partial_x f - E \partial_v f = \nu_{ee} \partial_v [(v - u) f + T \partial_v f] , \\ -\partial_{xx} \phi = n_i - n, \quad E = -\partial_x \phi, \end{cases}$$

with $\nu_{ee} = 0.01$, which corresponds to a weakly collisional plasma. Also the background ion density is considered as time-independent and given by

$$n_i(x) = 1 + \kappa \cos(kx), \quad \forall x \in (0, L),$$

with $k = 2\pi/L$, $L = 12$ and $\kappa = 0.1$, whereas the electron initial distribution function f_0 is given by

$$(5.1) \quad f_0(x, v) = \frac{1}{6\sqrt{2\pi}} (1 + 5v^2) \exp\left(-\frac{|v - u_0(x)|^2}{2}\right), \quad \forall (x, v) \in (0, L) \times \mathbb{R},$$

with $u_0(x) = 0.5 \sin(kx)$. Let us emphasize that the distribution function f is initially far from the thermal equilibrium since it corresponds to two streams in the velocity variable with a nonzero mean velocity u_0 . Moreover, since we do not consider in this test case collisions between electrons and ions, this equation conserves mass, momentum and total energy, hence the assumption that

$$\int_0^L \int_{\mathbb{R}} v f_0^\varepsilon(x, v) dv dx = 0,$$

is mandatory to get the convergence of the distribution function, when $t \rightarrow \infty$, towards a stationary state given by the Maxwell-Boltzmann distribution (3.8). The scaling parameter necessary for the definition of the Hermite basis functions is chosen as $v_{th} = \sqrt{\bar{T}}$, where the temperature \bar{T} and the potential $\bar{\phi}$ correspond to the stationary solution of the limit model

$$(5.2) \quad \begin{cases} \frac{\mathfrak{N}}{2} \bar{T} + \frac{1}{2} \int_{\mathbb{T}} |\partial_x \bar{\phi}(x)|^2 dx = \mathfrak{E}, \\ -\partial_{xx} \bar{\phi} + c \exp\left(\frac{\bar{\phi}}{\bar{T}}\right) = n_i, \end{cases}$$

with c uniquely determined by the conservation of the particle number. This latter system has to be solved initially.

We performed several numerical simulations using the discontinuous Galerkin/Hermite method and refining the mesh and the time step Δt as in [16, 17], but for the sake of clarity we only report numerical simulations with $N_x \times N_H = 32 \times 64$ and $\Delta t = 1/500$ for which the numerical results are similar with those obtained with refined meshes. Since initially the solution is far from equilibrium and collective effects dominate, the adiabatic asymptotics is not valid in a transient regime, hence a large number of modes N_H is needed to describe kinetic effects. On one hand, we show on Figure 1 (a) the time evolution of the deviations with respect to the initial condition of the discrete mass, momentum and total energy and observe that the errors on these quantities are of order 5×10^{-8} (our space/time discretization does not ensure exact conservations) which is acceptable. We also present in Figure 1 (b) the convergence in time of the potential Φ towards its equilibrium $\bar{\Phi}$. The amplitude of the potential Φ first oscillates strongly, and then, for times $t \geq 20$, it is damped and converges to the stationary state $\bar{\Phi}$ given by (5.2).

On the other hand, we present in Figure 2 (a) the time evolution of the L^2 -norm of the mean

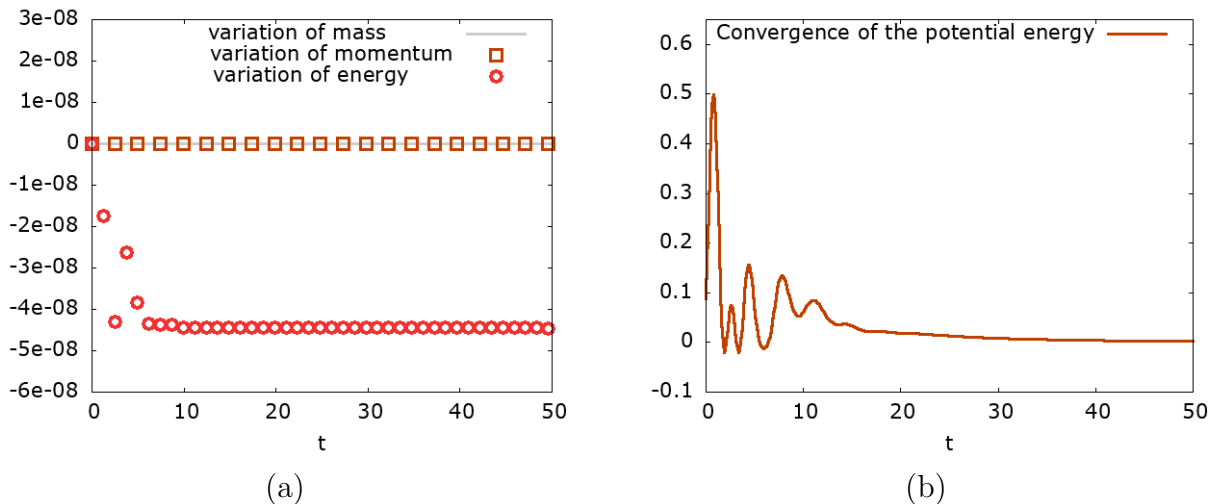


FIGURE 1. **One species case** : (a) deviation of mass, momentum and energy as compared to the initial condition; (b) time evolution of the potential deviations from the asymptotic value $\bar{\Phi}$ for $N_x \times N_H = 32 \times 64$.

electron velocity as well as of the temperature-deviation with respect to the temperature equilibrium v_{th}^2 in log scale. As for the potential, we observe a transient regime, where collective effects dominate, then both quantities converge to zero exponentially fast. In Figure 1(b) we present then the time evolution of the L^2 -norm of the Hermite coefficients $(\alpha_k)_{1 \leq k \leq 6}$. All these coefficients decrease almost exponentially fast to zero, saturating then around 10^{-12} . This illustrates the convergence of our electron distribution function (when $t \rightarrow \infty$) towards the Maxwell-Boltzmann distribution for which all Hermite coefficients are zero, except the main one α_0 . This is made possible by the appropriate choice of the scaling parameter $v_{th} = \sqrt{T}$ according to (5.2). These results show that in practice, higher-order Hermite coefficients can be neglected when t becomes large and thus the truncated Hermite hierarchy reduces to a constant approximation of the limit system (3.8)-(3.12). It illustrates the efficiency of our algorithm passing automatically from the numerical resolution (and complexity) of the kinetic equation when the solution is far from a Maxwell-Boltzmann distribution to the adiabatic limit, where only one mode is used for the density.

Finally we show on Figure 3 some snapshots of the electron distribution function corresponding to the transient regime. Indeed, when $t \leq 12.5$, collective effects dominate and the distribution function starts to develop some filaments in phase space then for larger times the electric field is damped (due to collisional effects) and f converges to the space non homogeneous Maxwell-Boltzmann equilibrium when $t \rightarrow \infty$.

5.2. Two species case. In this second test case we consider the multi-species framework, which is more relevant in plasma physics but to reduce the computational effort we design a simplified version of the two species case. Indeed, due to the fact that the present scheme does not cope with the time-stiffness, we have to adapt the time-step Δt with the electron dynamics, thus choosing $\Delta t \sim \varepsilon$. This leads (in general) to rather huge computational costs for the resolution of the kinetic ion dynamics for small ε -values, the electron dynamics being not so cumbersome, due to the well-designed Hermite approach. Hence, to be able to perform some simulations in reasonable times, we shall suppose here the ions well-defined by macroscopic quantities, and uniquely the electrons follow a kinetic model. This shall greatly

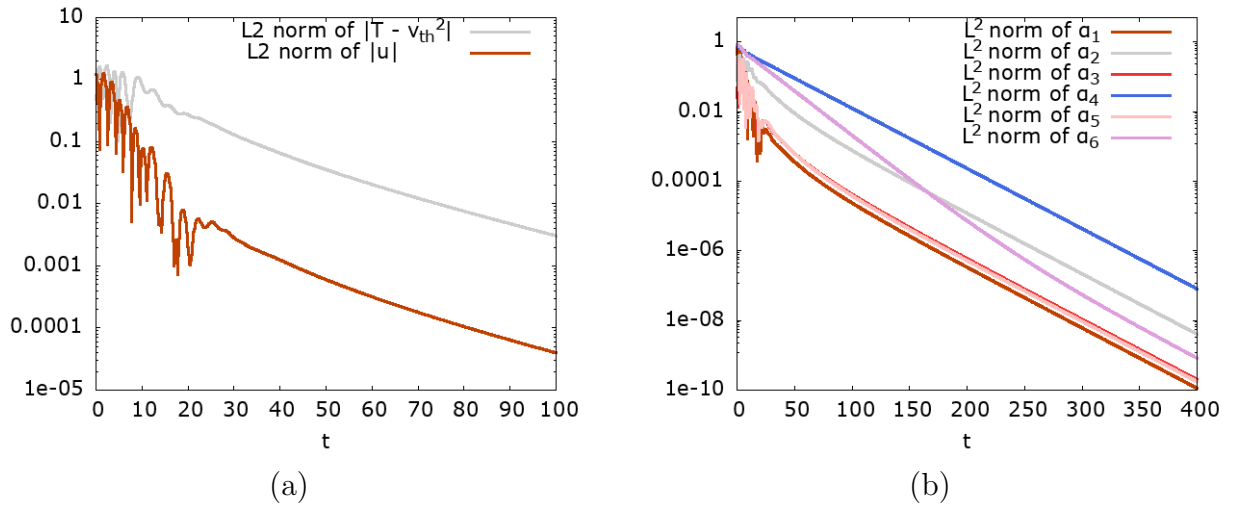


FIGURE 2. **One species case:** (a) time evolution (in log-scale) of $\|u\|_{L^2}$ and $\|T - v_{th}^2\|_{L^2}$; (b) time evolution of the Hermite-coefficients $(\alpha_k)_{1 \leq k \leq 6}$ in log-scale, for $N_x \times N_H = 32 \times 64$.

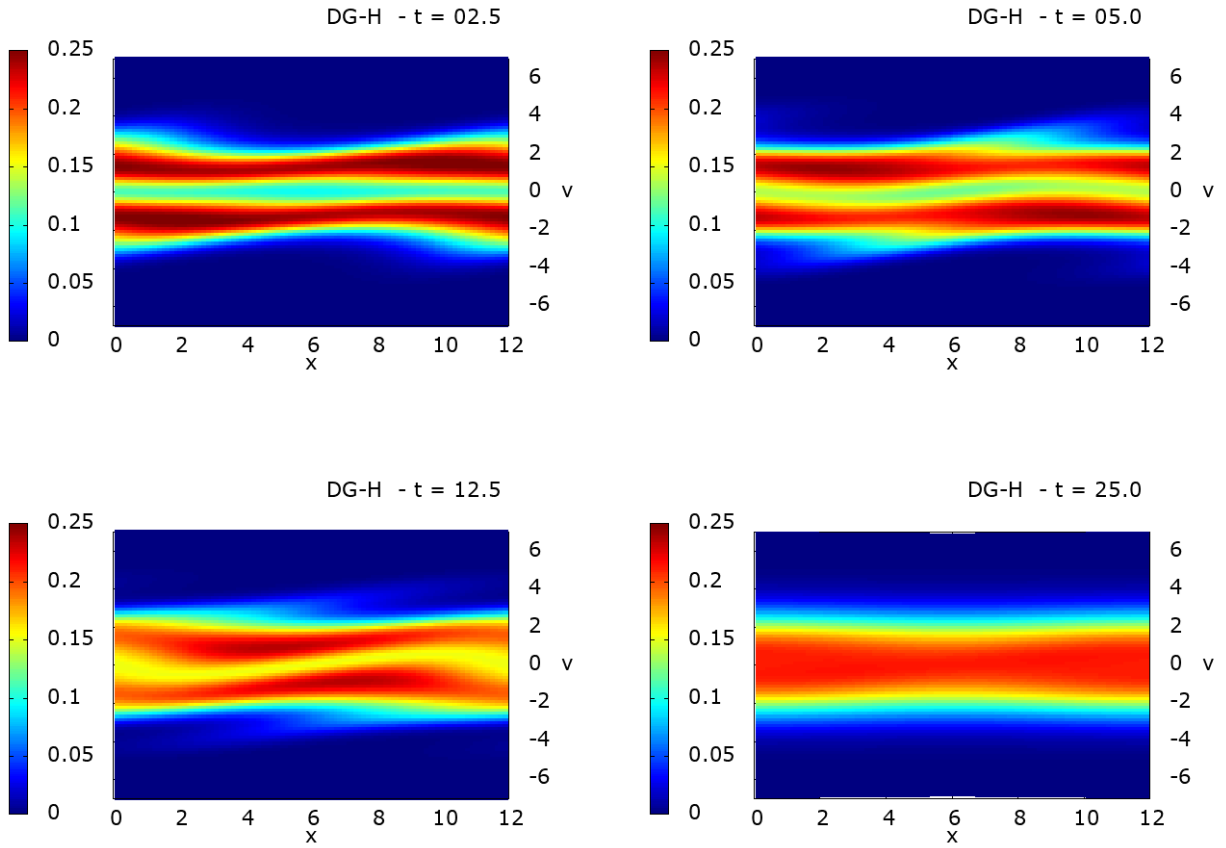


FIGURE 3. **One species case:** Surface plot of the distribution function f at several times $t = 2.5, 5, 12.5$ and 25 , with $N_x \times N_H = 32 \times 64$.

accelerate the computations, and shall permit to focus on the adiabatic electron asymptotics, and the designed Hermite spectral approach.

Let us start by assuming the electron distribution function f_e being solution to the Vlasov-Poisson-Fokker-Planck equation (4.1) with $(\nu_{ee}, \nu_{ei}) = (0.5, 0.1)$ and an initial distribution given by

$$(5.3) \quad f_e(0, x, v) = \frac{1}{\sqrt{2\pi}} \exp\left(-\frac{v^2}{2}\right) (1 + \kappa \cos(kx)), \quad \forall (x, v) \in \mathbb{T} \times \mathbb{R},$$

with $\kappa = 0.01$ and $k = 2\pi/L$ with $L = 12$.

The ion distribution function is supposed Maxwellian

$$f_i(t, x, v) := \frac{n_i(x)}{\sqrt{2\pi T_i(t)}} e^{-\frac{v^2}{2T_i(t)}},$$

with a density depending only on the space variable and given by

$$n_i(x) = 1 + 0.2 \cos(kx), \quad \forall x \in \mathbb{T},$$

whereas the mean velocity u_i is set to zero and the ion temperature T_i is supposed to depend only on the time variable and to satisfy the following equation

$$-\varepsilon \mathbf{n}_e \frac{dT_i}{dt} = \iint_{\mathbb{T} \times \mathbb{R}} \mathcal{Q}_{ei}(f_e) |v|^2 dv dx.$$

The choice of the right hand side in the latter equation is motivated by the requirement of an exact conservation of the total energy. Indeed, multiplying (4.1) by $v^2/2$ and integrating with respect to $(x, v) \in \mathbb{T} \times \mathbb{R}$, yields

$$\begin{aligned} \frac{\varepsilon}{2} \frac{d}{dt} \iint_{\mathbb{T} \times \mathbb{R}} f_e |v|^2 dv dx &= - \int_{\mathbb{T}} E n_e u_e dx + \frac{1}{2} \iint_{\mathbb{T} \times \mathbb{R}} \mathcal{Q}_{ei}(f_e) |v|^2 dv dx \\ &= - \int_{\mathbb{T}} \phi \partial_x (n_e u_e) dx + \int_{\mathbb{T}} \nu_{ei} n_e S_{ei} dx, \end{aligned}$$

where S_{ei} is given by (2.16). Furthermore using the continuity equation on n_e (2.15) and the fact that n_i does not depend on time, we have

$$\varepsilon \partial_t (n_e - n_i) + \partial_x (n_e u_e) = 0,$$

such that using Poisson's equation and the equation for T_i , permits indeed to obtain the total energy conservation

$$\frac{\varepsilon}{2} \frac{d}{dt} \left[\iint_{\mathbb{T} \times \mathbb{R}} f_e |v|^2 dv dx + \int_{\mathbb{T}} |E|^2 dx + \mathbf{n}_e T_i \right] = 0.$$

Remark 5.1. *Observe that similarly to T_i , we could also impose an equation on the mean velocity u_i to conserve the global momentum, but it is not necessary for our purpose here.*

Now let us verify that for this simplified model, the distribution function f_e tends to the Maxwell-Boltzmann distribution (3.8) when $\varepsilon \rightarrow 0$. The point is that the simplified model does not satisfy the H-theorem for any $\varepsilon > 0$, but we will show that it is verified when ε is sufficiently small provided that the macroscopic quantities are bounded. Indeed, computing

the time derivative of the entropy gives

$$\begin{aligned} \varepsilon \frac{d}{dt} \iint_{\mathbb{T} \times \mathbb{R}} f_e \log(f_e) dv dx &+ \iint_{\mathbb{T} \times \mathbb{R}} \left[\nu_{ee} T_{ee} \frac{\mathcal{M}_e}{h_e} |\partial_v h_e|^2 + \nu_{ei} T_{ei} \frac{\mathcal{M}_{ei}}{h_{ei}} |\partial_v h_{ei}|^2 \right] dv dx \\ &= \iint_{\mathbb{T} \times \mathbb{R}} \frac{\nu_{ei}}{T_{ei}} (f_e |v - u_{ei}|^2 - T_{ei} f_e) dv dx, \end{aligned}$$

where h_e and h_{ei} are given in (2.11). Then, computing the term on the right hand side yields

$$\begin{aligned} \varepsilon \frac{d\mathcal{H}_e}{dt} &+ \iint_{\mathbb{T} \times \mathbb{R}} \left[\nu_{ee} T_{ee} \frac{\mathcal{M}_e}{h_e} |\partial_v h_e|^2 + \nu_{ei} T_{ei} \frac{\mathcal{M}_{ei}}{h_{ei}} |\partial_v h_{ei}|^2 \right] dv dx \\ (5.4) \quad &= -\frac{1 - \varepsilon^2}{1 + \varepsilon^2} \int_{\mathbb{T}} \frac{\nu_{ei} n_e |u_e|^2}{4 T_{ei}} dx + \frac{\varepsilon^2}{1 + \varepsilon^2} \int_{\mathbb{T}} \frac{\nu_{ei} n_e}{T_{ei}} (T_e^\varepsilon - T_i) dx. \end{aligned}$$

Therefore, in the limit $\varepsilon \rightarrow 0$, we can proceed as in the proof of Theorem 3.1 and get, from the entropy dissipation, that in the limit f_e tends towards an equilibrium of the form $\mathcal{M}_{n_e, 0, T_e}$ where n_e is given by (3.8). Furthermore, using the definition of S_{ei} in (2.16), the equation on T_i can be written as

$$\mathbf{n}_e \frac{dT_i}{dt} = \frac{2\varepsilon}{1 + \varepsilon^2} \int_{\mathbb{T}} \nu_{ei} n_e \left[T_e - T_i + \frac{|u_e|^2}{2} \right] dx,$$

which means that T_i converges to a constant temperature as $\varepsilon \rightarrow 0$. Let us mention that a similar approach has been used in [5] in a slightly different context.

After this short presentation of our simplified model, let us present our numerical results. We take $N_x \times N_H = 32 \times 32$ and compare the obtained solutions with a reference solution computed on a refined grid of $N_x \times N_H = 128 \times 128$ for several values of $\varepsilon \in \{10^{-3}, 10^{-2}, 10^{-1}, 1\}$. The scaling parameter v_{th} in (4.20) is chosen so that the numerical scheme captures the asymptotic behavior of the solution f_e when $\varepsilon \rightarrow 0$. Since the initial data is far from the Maxwell-Boltzmann equilibrium, the time step is initially chosen proportional to ε as $\Delta t = \varepsilon/500$ whereas we choose $N_x = N_H = 32$.

We show first the numerical results for $\varepsilon = 10^{-3}$. On one hand, we present on Figure 4 (a) the time evolution of the deviations of the discrete mass and total energy, when compared with the initial values. Here, the errors on mass and total energy are of order 10^{-7} . We remind that our space discretization does not ensure exact conservation of energy but their variations remain very small during the simulation. On the other hand, we present the time evolution of the L^2 -norm of the first Hermite coefficients $(\alpha_k)_{1 \leq k \leq 6}$ in Figure 4 (b). For $k \geq 1$, the L^2 -norm of these coefficients decreases almost exponentially fast and oscillates. These numerical results illustrate the efficiency of our approach based on the Hermite decomposition of the distribution function f_e , when treating situations with $\varepsilon \ll 1$. Indeed, for $\varepsilon \rightarrow 0$ all coefficients $(\alpha_k)_{k \geq 1}$ converge to zero very rapidly as $e^{-Ct/\varepsilon}$, hence after a short transient regime, the numerical solution can be approximated very well with only few Hermite coefficients, the Maxwell-Boltzmann distribution corresponding to only one coefficient α_0 . Once again, our Hermite decomposition is particularly well adapted to this asymptotic regime since the number of modes may be adapted along the simulation by neglecting the Hermite coefficients of smaller amplitudes [36]. The main issue remains however to develop an efficient time discretization avoiding the ε -dependent constraint on the time step.

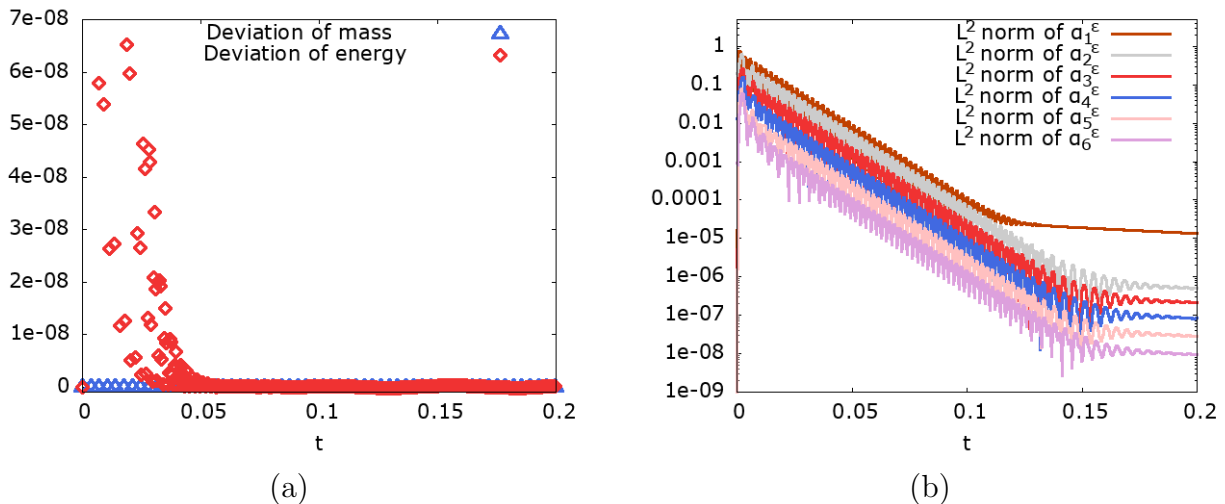


FIGURE 4. **Two species case** ($\varepsilon = 10^{-3}$): (a) deviation of mass and energy with respect to the initial condition; (b) time evolution of the L^2 norm of the Hermite coefficients $(\alpha_k)_{1 \leq k \leq 6}$ in logarithmic scale for $N_x \times N_H = 32 \times 32$.

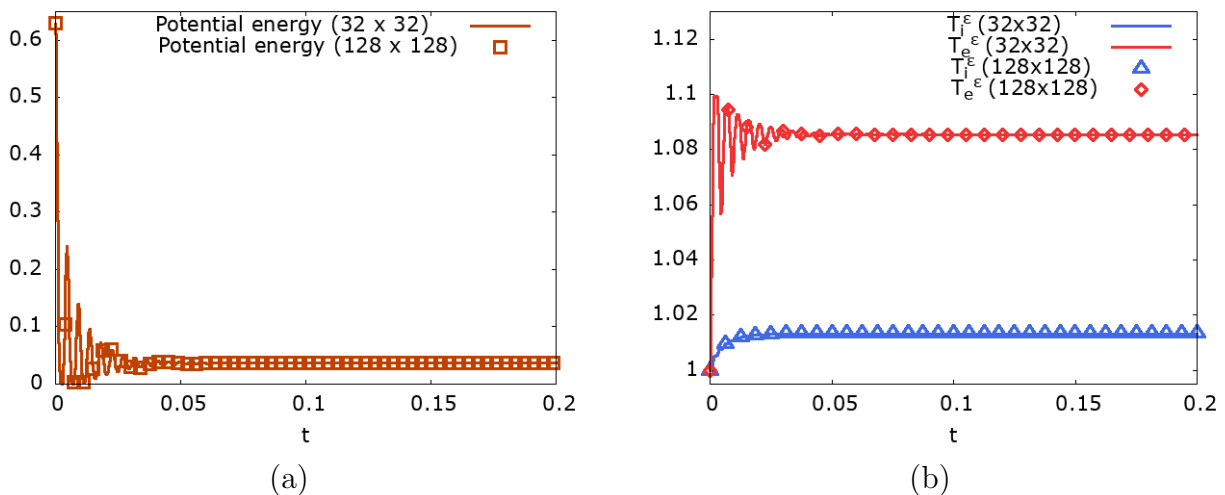


FIGURE 5. **Two species case** ($\varepsilon = 10^{-3}$): (a) time evolution of the potential energy, (b) time evolution of the global temperatures T_e and T_i with $N_x \times N_H = 32 \times 32$, whereas the reference solution is with $N_x \times N_H = 128 \times 128$.

We also plot the time evolution of the potential energy and of the global temperatures (averaged in space) of the electrons and ions in Figure 5. We compare them to the results obtained with a refined mesh of size 128×128 and we can see that these results have the same structure. This means that with coarse grids we already get satisfactory results. Furthermore, we observe that the potential energy oscillates in time and is damped until it reaches a stationary state. The electron temperature has a similar behavior whereas the ion temperature grows until it converges finally also towards a stationary state.

Finally in order to illustrate the convergence to the Maxwell-Boltzmann distribution, we show some snapshots of the electron density n_e and of the electric potential ϕ in Figure 6. Both quantities converge, after an oscillatory transient region, towards their equilibrium corresponding to (3.8)-(3.12).

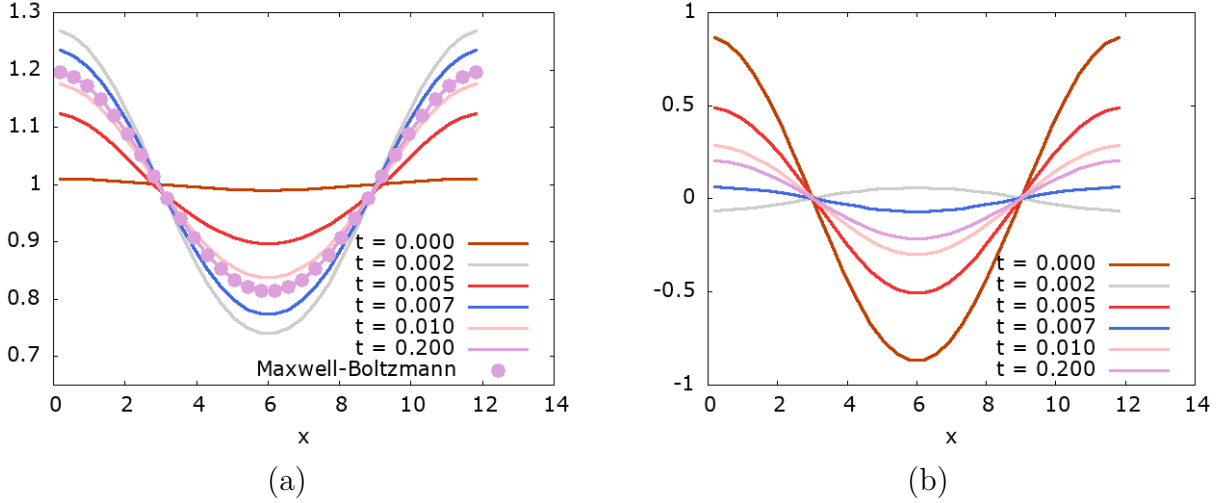
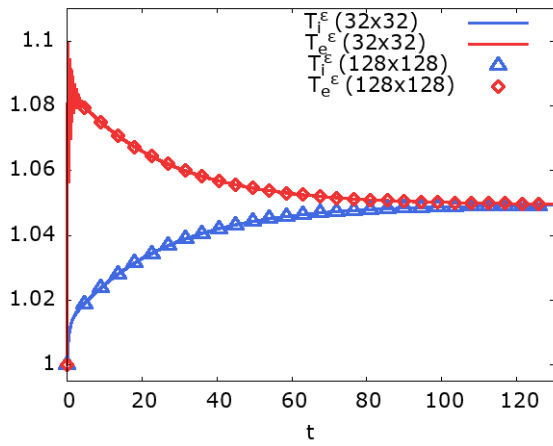


FIGURE 6. **Two species case** ($\varepsilon = 10^{-3}$): plot of the (a) electron density n_e and (b) electric potential ϕ at different times and with $N_x \times N_H = 32 \times 32$.

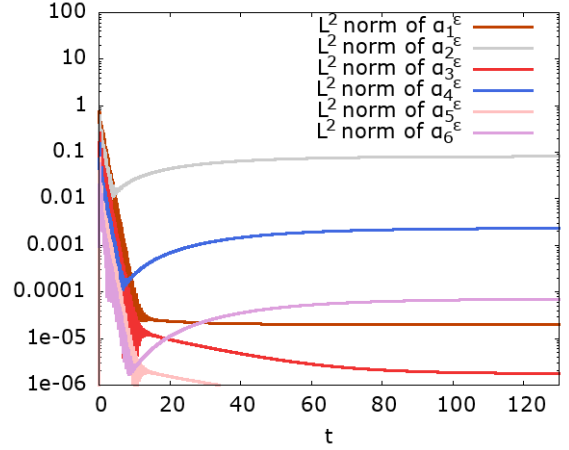
Next we performed some computations for other values of $\varepsilon > 0$. We get similar results concerning the mass and energy variations. To illustrate the different regimes, we present in Figure 7, the time evolution of the electron temperature T_e resp. ion temperature T_i as well as of the Hermite coefficients $(\alpha_k)_{1 \leq k \leq 6}$ for $\varepsilon = 10^{-1}$ and $\varepsilon = 1$. For such large values of ε we are no more close to the Maxwell-Boltzmann regime. When t becomes larger, the solution f_e of (4.1) converges to a steady state, and both temperatures, after oscillating, tend towards a stationary state. When $\varepsilon = 1$ (and $\nu_{ee} = 0.1$), the electronic temperature strongly oscillates, then it approaches an equilibrium at $t \simeq 40$. However, for $\varepsilon = 0.1$, oscillations are rapidly damped and the cooling process is much slower than in the previous case, in particular T_e approaches its equilibrium at $t \simeq 120$. This point comes from the fact that the temperature equilibration is ε -dependent, and for smaller and smaller ε values, the equilibration of the ion and electron temperatures get slower and slower, however, for each $\varepsilon > 0$ both temperatures converge towards the same value in the long-time limit.

Concerning the Hermite coefficients, they first oscillate with a damping amplitude, but after a while they stabilize ($\varepsilon = 1$) or increase slowly ($\varepsilon = 10^{-1}$). This underlines the fact that even if the solution f converges to an equilibrium when t goes to infinity, this equilibrium does not coincide with the Maxwell-Boltzmann distribution obtained when $\varepsilon \rightarrow 0$. The two limits are different in the here presented test case. Therefore, the solution cannot be represented by only one coefficient (α_0) but higher-order even coefficients are mandatory during the simulations whereas odd coefficients converge to zero.

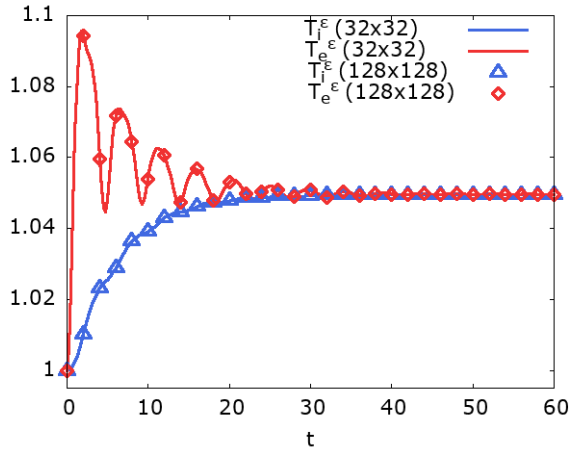
However, we observe that most coefficients decrease rapidly to zero and the efficiency of the adaptive algorithm proposed in Section 4.3 is illustrated in Figure 8, where we present the time evolution of the number of considered Hermite functions for various values of ε , ranging from 10^{-3} to 1. As expected, when ε is small ($\varepsilon = 10^{-3}$ or 10^{-2}), the solution converges rapidly to the Maxwell-Boltzmann distribution after a short initial time layer and f can be approximated with very few Hermite coefficients ($0 \leq k \leq 2$ since we apply the adaptive algorithm only for $k \geq 3$). For larger values of ε , the solution does not match with the Maxwell-Boltzmann distribution and the number of Hermite coefficients oscillates according to the variations of the distribution function, but after some time only a small number of



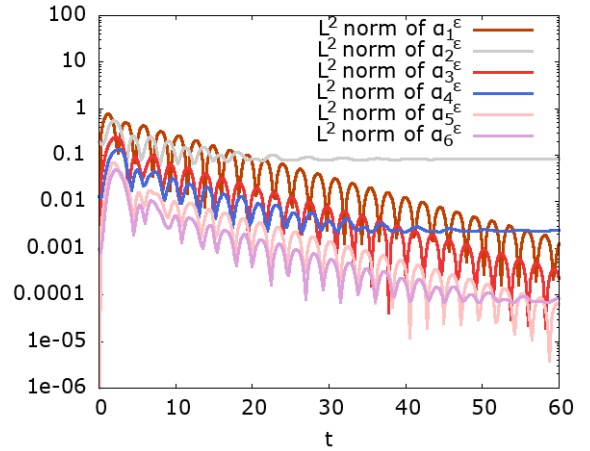
(a) Temperature ($\varepsilon = 0.1$)



(b) $(\alpha_k)_{1 \leq k \leq 6}$ ($\varepsilon = 0.1$)



(c) Temperature ($\varepsilon = 1$)



(d) $(\alpha_k)_{1 \leq k \leq 6}$ ($\varepsilon = 1$)

FIGURE 7. **Two species case** $\varepsilon = 0.1$ and $\varepsilon = 1$: time evolution of (left) the global temperatures T_e and T_i (right) the L^2 norm of the Hermite coefficients $(\alpha_k)_{1 \leq k \leq 6}$ in logarithmic value.

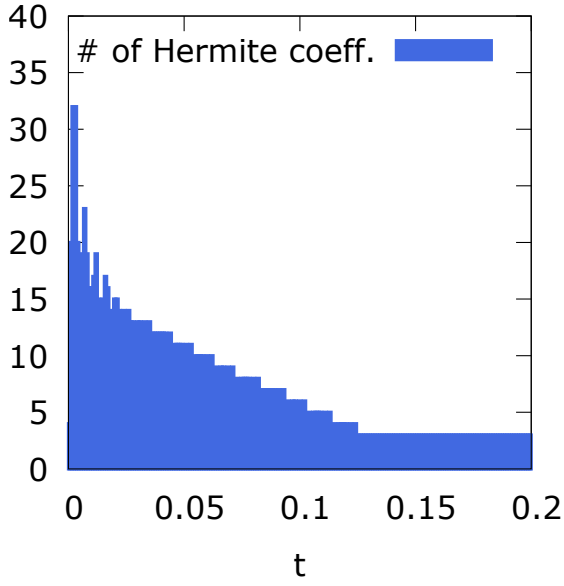
coefficients are finally used ($0 \leq k \leq 5$). This algorithm allows to reduce drastically the computational time for various regimes.

6. CONCLUDING REMARKS AND PERSPECTIVES

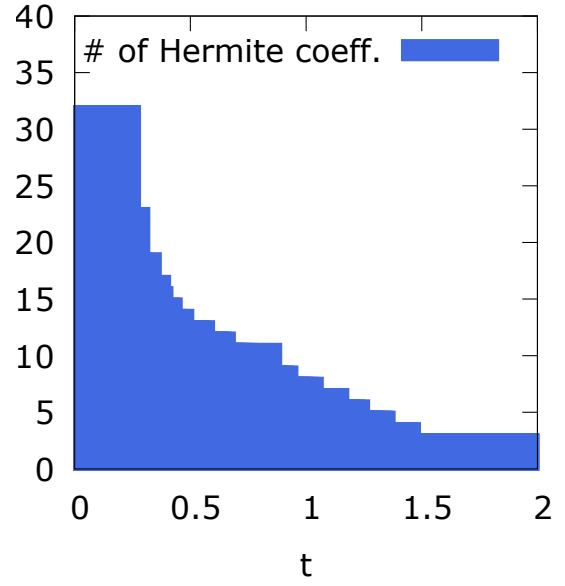
Let us conclude this paper by summarizing what was achieved in this work and what remains still to be done in future works.

The focus of this paper was the introduction of mixed Fokker-Planck collision operators taking into account especially for ion-electron collisions in thermonuclear fusion plasmas, and satisfying the desired physical properties as the three conservation laws and the entropy-decay relation. Based on these new operators, a second aim was to study the adiabatic electron limit $\varepsilon \rightarrow 0$, where the small parameter ε stands somehow for the electron-to-ion mass ratio. The small ε -regime corresponds to the description of phenomena occurring at ion scales, whereas the rapid electrons are thermalized and approximated via macroscopic models (adiabatic Boltzmann relation).

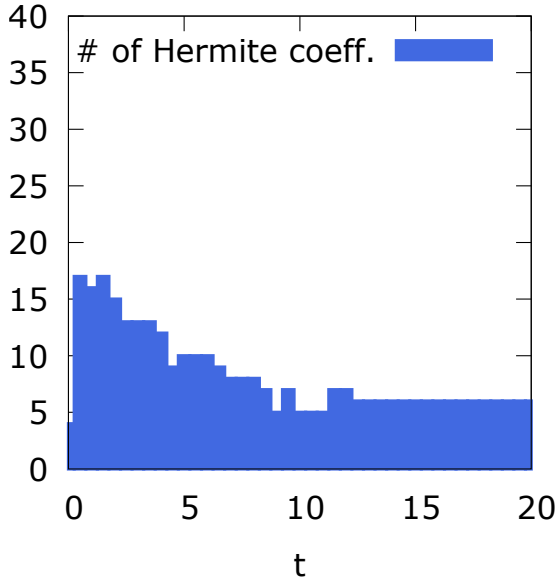
A formal asymptotic limit $\varepsilon \rightarrow 0$ permitted to obtain the macroscopic model satisfied by the thermalized electrons. During this limit the ions remain kinetic. Then a first numerical



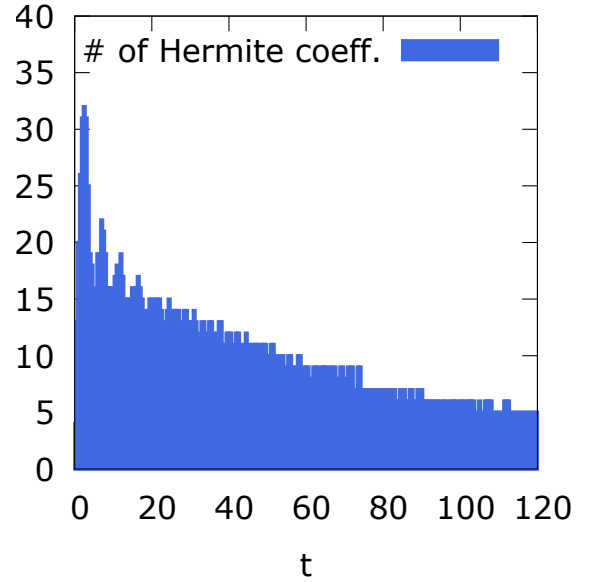
(a) $\varepsilon = 10^{-3}$



(b) $\varepsilon = 10^{-2}$



(c) $\varepsilon = 10^{-1}$



(d) $\varepsilon = 1.$

FIGURE 8. **Two species case** : time evolution of the number of considered Hermite coefficients when Algorithm 1 is applied for different values of ε .

scheme was proposed in order to solve the Vlasov-Poisson-Fokker-Planck system, based on a Hermite spectral method in the velocity variable and a discontinuous Galerkin method in the space variable.

One of the main difficulties when trying to solve numerically the Vlasov-Poisson Fokker-Planck system (3.1)-(3.3) in the small ε -regime is the singularity of the problem. The advantage of choosing a Hermite spectral method (to discretize the velocity variable) with a suitable choice of the weights, is that in the small ε -regime only few modes have to be taken into account. This reduces drastically the computational costs. Indeed, an exact Maxwellian,

as our limiting adiabatic distribution function, is fully represented by only one mode in the Hermite expansion, if the scaling is well adapted. Thus the transition from the kinetic to the adiabatic model is somehow intrinsic to this Hermite spectral approach.

There remain however still several points to be treated in future works, to render the method more efficient. For example for weakly collisional plasmas, the dissipation is not sufficiently large and the time step still depends on ε , only the Hermite-approach permitted to render the computations more tractable for the electrons. A *multi-scale* approach is one of our next aims on the way to get more performant methods in the study of this two-species adiabatic limit, in particular to be able to adapt dynamically the time step (initial layer, equilibrium regime) or to choose ε -independent grids. Furthermore, a tricky discretization of the Limit-model, permitting to compute efficiently the scaling factor $v_{th}(t)$, is also a complex task to be achieved. And finally, after all these improvements, a full ion/electron computation shall become possible and has to be completed in a real physical situation [15].

Acknowledgments. This work has been carried out within the framework of the EUROfusion Consortium, funded by the European Union via the Euratom Research and Training Programme (Grant Agreement No 101052200 — EUROfusion). Views and opinions expressed are however those of the author(s) only and do not necessarily reflect those of the European Union or the European Commission. Neither the European Union nor the European Commission can be held responsible for them.

REFERENCES

- [1] P. Andries, K. Aoki, and B. Perthame, *A consistent bgk-type model for gas mixtures*, Journal of Statistical Physics, **106** (2002), pp. 993–1018.
- [2] B. Ayuso, J. A. Carrillo and C. W. Shu, *Discontinuous Galerkin methods for the multi-dimensional Vlasov–Poisson problem*, Mathematical Models and Methods in Applied Sciences, **22**, (2021) pp. 1250042.
- [3] A. Bobylev, M. Bisi, M. Groppi and G. Spiga, I. Potapenko, *A general consistent BGK model for gas mixtures*, Kinet. Relat. Models **11** (2018), no. 6, 1377–1393.
- [4] A. V. Bobylev and I.F. Potapenko, *Long wave asymptotics for the Vlasov–Poisson–Landau kinetic equation*, J. Stat. Phys. **175** (2019), no. 1, 1–18
- [5] C. Buet, S. Dellacherie and R. Sentis, *Numerical solution of an ionic Fokker–Planck equation with electronic temperature*, SIAM J. Numer. Anal. **39** (2001), no. 4, 1219–1253.
- [6] K.L. Cartwright, J. P. Verboncoeur and C. K. Birdsall, *Nonlinear hybrid Boltzmann-particle-in-cell acceleration algorithm*, Physics of Plasmas (1994-present), **7.8** (2000): 3252–3264.
- [7] F. F. Chen, *Plasma Physics and controlled fusion*, Springer Verlag New York, (2006).
- [8] Y. Chen, S. Parker, *A gyrokinetic ion zero electron inertia fluid electron model for turbulence simulations*, Phys. Plasmas **8**, no. 2, 441–446 (2001)
- [9] B. Cockburn, G. E. Karniadakis and C. W. Shu, *The development of discontinuous Galerkin methods*, (Newport, RI, 1999), Lect. Notes Comput. Sci. Eng., **11**, Springer, Berlin, 2000.
- [10] N. Crouseilles and F. Filbet, *Numerical approximation of collisional plasmas by high order methods*, J. Comput. Phys. **201** (2004), no. 2, 546–572.
- [11] P. Degond, *Chapter 1 - Asymptotic Continuum Models for Plasmas and Disparate Mass Gaseous Binary Mixtures*, in Material Substructures in Complex Bodies, edited by Gianfranco Capriz Paolo Maria Mariano, Elsevier Science Ltd, Oxford, 2007, Pages 1-62.
- [12] R. Duclous, B. Dubroca, F. Filbet and V. Tikhonchuk, *High order resolution of the Maxwell-Fokker-Planck-Landau model intended for ICF applications*, J. Comput. Phys. **228** (2009), no. 14, 5072–5100.
- [13] Y. Di, Y. Fan, Z. Kou, R. Li, Y. Wang, *Filtered hyperbolic moment method for the Vlasov equation*, J. Sci. Comput. **79** (2019) 969–991.

- [14] J. Dominski, S. Brunner, S.K. Aghdam, T. Goerler, F. Jenko, D.Told *Identifying the role of non-adiabatic passing electrons in ITG/TEM microturbulence by comparing fully kinetic and hybrid electron simulations*, Journal of Physics: Conference Series **401** (2012).
- [15] F. Filbet and C. Negulescu, *Asymptotic preserving scheme for Fokker-Planck multi-species equations in the adiabatic asymptotics*, In preparation (2022).
- [16] F. Filbet and T. Xiong, *Conservative Discontinuous Galerkin/Hermite Spectral Method for the Vlasov-Poisson System*, Commun. Appl. Math. Comput. , 2020
- [17] F. Filbet and M. Bessemoulin-Chatard, *On the stability of conservative discontinuous Galerkin/Hermite Spectral methods for the Vlasov-Poisson System*, J. Comp. Physics, 2022
- [18] D. Han-Kwan and F. Rousset, *Quasi-neutral limit for Vlasov-Poisson with Penrose stable data* Ann. Sci. École Norm. Sup. **49**, pp. 1445–1495 (2016)
- [19] X. Garbet et al., *Global simulations of ion turbulence with magnetic shear reversal*, Physics of Plasmas (1994-present) **8.6** (2001): 2793-2803.
- [20] R. J. Goldston, P. H. Rutherford, *Plasma Physics*, Taylor & Francis Group, (1995).
- [21] H. Goedbloed, S. Poedts, *Principles of Magnetohydrodynamics*, Cambridge University Press, Cambridge, (2004).
- [22] H. Grad, On the kinetic theory of rarefied gases, *Comm. Pure Appl. Math.* **2** (1949), 331–407.
- [23] J. Greene, *Improved Bhatnagar-Gross-Krook model of electron-ion collisions*. Phys. Fluids **16**, 2022–2023 (1973)
- [24] E. P. Gross and M. Krook, *Model for collision processes in gases: Small-amplitude oscillations of charged two-component systems*, Phys. Rev., **102** (1956), pp. 593–604,
- [25] R.D. Hazeltine, *Rotation of a toroidally confined, collisional plasma*, Physics of Fluids (1958-1988) **17.5** (1974): 961-968.
- [26] B. B. Hamel, *Kinetic model for binary gas mixtures*, Physics of Fluids, **8** (1965), pp. 418–425,
- [27] R.D. Hazeltine, J.D. Meiss, *Plasma confinement*, Dover Publications, Inc. Mineola, New York (2003).
- [28] F. L. Hinton and R. D. Hazeltine, *Theory of plasma transport in toroidal confinement systems*, Reviews of Modern Physics **48.2** **23** (1976).
- [29] M. Herda and L. M. Rodrigues, *Anisotropic Boltzmann-Gibbs dynamics of strongly magnetized Vlasov-Fokker-Planck equations* Kinet. Relat. Models **12** (2019), no. 3, 593–636.
- [30] C. Klingenberg, M. Pirner, and G. Puppo, *A consistent kinetic model for a two-component mixture with an application to plasma*, Kinetic and Related Models, **10** (2017), pp. 445–465,
- [31] D. T. K. Kwok, *A hybrid Boltzmann electrons and PIC ions model for simulating transient state of partially ionized plasma*, Journal of Computational Physics **227.11** (2008): 5758-5777.
- [32] C. Negulescu, "Kinetic modelling of strongly magnetized tokamak plasmas with mass disparate particles. The electron Boltzmann relation.", SIAM MMS (Multiscale Model. Simul.) **16** (2018), no. 4, 1732–1755.
- [33] R. Li, Y. Ren, Yinuo, Y. Wang, *Hermite spectral method for Fokker-Planck-Landau equation modeling collisional plasma*, J. Comput. Phys. **434** (2021).
- [34] J.W. Schumer, J.P. Holloway, *Vlasov simulations using velocity-scaled Hermite representations*, J. Comput. Phys. **144** (2) (1998) 626–661.
- [35] W. T. Taitano, B. D. Keenan, L. Chacón, S. E. Anderson, H. R. Hammer, A. N. Simakov, *An Eulerian Vlasov-Fokker-Planck algorithm for spherical implosion simulations of inertial confinement fusion capsules* Comput. Phys. Commun. **263** (2021), Paper No. 107861, 42 pp.
- [36] J. Vencels, G.L. Delzanno, A. Johnson, I.B. Peng, E. Laure and S. Markidis, *Spectral solver for multi-scale plasma physics simulations with dynamically adaptive number of moments* Procedia Computer Science, **51**, (2015) pp.1148-1157.

UNIVERSITÉ DE TOULOUSE & CNRS, UPS, INSTITUT DE MATHÉMATIQUES DE TOULOUSE UMR 5219, F-31062 TOULOUSE, FRANCE.

Email address: francis.filbet@math.univ-toulouse.fr, claudia.negulescu@math.univ-toulouse.fr